Research Paper

GEOSPHERE

GEOSPHERE; v. 12, no. 2

doi:10.1130/GES01257.1

11 figures; 1 table; 1 supplemental file

CORRESPONDENCE: chapman@macalester.edu

CITATION: Chapman, A.D., Jacobson, C.E., Ernst, W.G., Grove, M., Dumitru, T., Hourigan, J., and Ducea, M.N., 2016, Assembling the world's type shallow subduction complex: Detrital zircon geochronologic constraints on the origin of the Nacimiento block, central California Coast Ranges: Geosphere, v. 12, no. 2, p. 533–557, doi:10.1130/GES01257.1.

Received 28 August 2015
Revision received 14 November 2015
Accepted 28 January 2016
Published online 29 February 2016

Assembling the world's type shallow subduction complex: Detrital zircon geochronologic constraints on the origin of the Nacimiento block, central California Coast Ranges

Alan D. Chapman[1,2], Carl E. Jacobson[3], W.G. Ernst[1], Marty Grove[1], Trevor Dumitru[1], Jeremy Hourigan[4], and Mihai N. Ducea[5]

[1]Department of Geological Sciences, Stanford University, Stanford, California 94305, USA
[2]Geology Department, Macalester College, St. Paul, Minnesota 55105, USA
[3]Department of Geological and Atmospheric Sciences, Iowa State University, Ames, Iowa 50011, USA
[4]Department of Earth and Planetary Sciences, University of California, Santa Cruz, California 95064, USA
[5]Department of Geosciences, University of Arizona, Tucson, Arizona 85721, USA

ABSTRACT

Temporal and spatial patterns in the architecture of the Franciscan Complex provide valuable insights into the subduction processes through which such patterns arise. The Nacimiento Franciscan belt is an allochthonous sliver of subduction assemblages in the central California Coast Ranges displaced either: (1) from southern California by >300 km of Neogene dextral slip along the San Andreas fault system or (2) from central California to southern California and back again, by >500 km of Late Cretaceous–Paleocene sinistral slip along the Sur-Nacimiento fault followed by San Andreas–related motion. New U-Pb detrital zircon data from 20 (meta)clastic samples indicate that the Nacimiento Franciscan section was assembled between ca. 95 and 80 Ma. Abundant Cretaceous (particularly Late Cretaceous) and diminishing amounts of Jurassic and Proterozoic zircon grains point to a southern California origin for Nacimiento Franciscan protoliths, precluding significant sinistral strike-slip along the Sur-Nacimiento fault. Furthermore, the suite of detrital zircon ages reported here bears a strong resemblance to new and existing data from subduction complexes in southern California that were emplaced during Laramide shallow subduction (i.e., Sierra de Salinas, Portal Ridge, Quartz Hill, Rand, San Emigdio, and Tehachapi schists). Hence, the Nacimiento Franciscan is distinct from Franciscan rocks in central and northern California and more likely represents an outboard element of the Late Cretaceous southern California low-angle subduction system. Upon restoring the Nacimiento block to its Late Cretaceous position, an inboard-younging trend is apparent in the composite Nacimiento–southern California schist belt, suggesting that progressively younger accretionary materials were underplated farther inboard by tectonic erosion. We posit that arc and forearc elements absent from southern California were removed by a combination of physical and tectonic erosion attending shallow subduction, interleaved in the subduction complex, and recycled into the mantle. Steepening of the Laramide slab was marked by a phase of crustal extension in the overriding plate. During this phase, the Sur-Nacimiento fault likely functioned as a segment of a low-angle normal fault system spanning the southern Sierra Nevada batholith to the Nacimiento accretionary system.

INTRODUCTION

The Franciscan Complex, exposed from central California to southern Oregon, is recognized as one of the most complete archives of subduction zone evolution in the world (e.g., Hamilton, 1969; Ernst, 1970). Geoscientific investigation of the Franciscan Complex has shed considerable light on how, and over what length and timescales, subduction accretion systems are assembled (e.g., by accretion and underplating), disassembled (e.g., by subduction erosion and trench-linked strike-slip faulting), and exhumed (Wakabayashi, 2015 and references therein). Profound along- and across-strike variations in accretionary belt character reflect the dynamic nature of Mesozoic subduction beneath western North America. For example, the northern Coast Ranges and San Francisco Bay Area contain a downward- and westward-younging (Early Cretaceous to middle Miocene) high-pressure/low-temperature (HP/LT) structural sequence juxtaposed with forearc sediments (Unruh et al., 2007; Ernst et al., 2009; Snow et al., 2010; Dumitru et al., 2010, 2015; Wakabayashi, 2015). In contrast, in southern California, high-pressure/high-temperature subduction assemblages appear to young along strike (Late Cretaceous to Eocene) and are juxtaposed with batholithic rocks with no intervening forearc (Jacobson et al., 1988; Jacobson et al., 1996; Grove et al., 2003; Saleeby, 2003; Kidder and Ducea, 2006; Chapman et al., 2011; Jacobson et al., 2011). These NW-SE variations are attributed to shallowing of the dip of the descending slab from northern to southern California (Saleeby, 2003; Liu et al., 2008, 2010).

Along-strike variations in strain partitioning from oblique subduction, resulting in domains variably affected by trench-linked strike-slip faulting, have also been proposed for the California subduction system (McLaughlin et al., 1988; Jayko and Blake, 1993). The Nacimiento Franciscan, a clearly allochthonous subduction assemblage exposed west of the San Andreas fault, is interpreted by some as having been displaced from its native site by >500 km of trench-linked sinistral slip (Dickinson, 1983; Dickinson et al., 2005; Jacobson et al., 2011; Singleton and Cloos, 2013). Other workers suggest minimal trench-parallel displacement within the Nacimiento Franciscan, instead positing that these rocks were thrust beneath Cretaceous forearc basin and batholithic rocks

in southern California (Page, 1970a, 1970b; Hall, 1991; Saleeby, 2003; Ducea et al., 2009; Hall and Saleeby, 2013). The origin of the Nacimiento Franciscan is disputed since, by comparison with the trench-forearc-arc triad east of the San Andreas fault, the juxtaposition of arc rocks of the Salinian block with Nacimiento assemblages along the Sur-Nacimiento fault implies the removal of a width of 150 km or greater of formerly intervening arc and forearc basin assemblages. Although general agreement exists that major displacements along this structure took place between 75 and 56 Ma (e.g., Dickinson et al., 2005; Jacobson et al., 2011), with late Cenozoic strike-slip remobilization linked to the San Andreas fault system (Hall, 1991), there is no consensus on the nature of Late Cretaceous to Paleocene slip along the fault.

The key aim here is to evaluate the thrust versus sinistral strike-slip models for the Sur-Nacimiento fault. In doing so, we will address the question of whether the Nacimiento Franciscan has a stronger affinity to the Franciscan Complex of central California or to Laramide shallow subduction[1] assemblages exposed in southern California. The models above are evaluated here using U-Pb detrital zircon geochronology and petrography, as each model predicts widely different protolith provenance. For example, a thrust origin for the Sur-Nacimiento fault predicts that Nacimiento Franciscan detritus was shed from the southern Sierra-Salinia–Mojave Desert region, whereas a sinistral origin predicts a detrital source outboard of the Diablo Range–San Francisco Bay Area with no intervening Salinian block (Jacobson et al., 2011). New palinspastic and geochronologic data from the Nacimiento Franciscan provide valuable constraints on the processes that controlled clastic deposition, structural assembly, tectonic erosion, and mélange formation in the Late Cretaceous California subduction system.

GEOLOGIC BACKGROUND

The sections that follow provide a geologic overview of the Nacimiento block, possibly correlative subduction assemblages in central and southern California, and the Sierra Nevada–Peninsular Ranges batholith. Figure 1 shows the current positions of these tectonic elements (inset) and a palinspastic map, modified after Grove et al. (2003) and Jacobson et al. (2011), that incorporates significant translational and rotational deformation, as a first-order approximation of geologic relations prior to initiation of slip on the San Andreas system. The reconstruction does not take into account: (1) new data suggesting that the Salinian block originated some 50–75 km farther south than is shown on the map (Sharman et al., 2013, 2015) given uncertainties about whether extra slip was accommodated along the San Andreas and San Gabriel faults or distributed through the Salinian block or (2) evidence for syn-subduction dextral slip along a "proto–San Andreas fault" (Page, 1981; Wakabayashi, 1999). Our palinspastic map differs from those listed above in that the San Rafael Mountains have not been back rotated in the manner of Dickinson (1996). Instead, we treat the Santa Ynez fault as separating relatively rotated (south) and nonrotated (north, including the San Rafael Mountains) domains in the western Transverse Ranges (e.g., Hornafius et al., 1986; Luyendyk, 1991).

[1]Throughout the manuscript, the term "shallow subduction" relates to the *angle*—not the *depth* of subduction. For example, "Laramide shallow subduction" or "shallow subduction assemblages" refer to a low angle of subduction in Laramide time and rocks carried into a shallow subduction zone, respectively.

Nacimiento Block

The Nacimiento block crops out over an ~300 × 30 km area in the central California Coast Ranges and is bounded to the east by the Sur-Nacimiento fault, to the south by the Santa Ynez fault, and to the west by the Pacific Ocean (Figs. 1 and 2). The block consists chiefly of subduction assemblages locally overlain by fragments of the Coast Range ophiolite along the Coast Range fault (Bailey et al., 1970; Ernst, 1970, 1980; Jayko et al., 1987; Dickinson et al., 2005; Hopson et al., 2008; Fig. 2). Ophiolitic assemblages are, in turn, unconformably overlain by forearc sedimentary rocks of the Great Valley Group, including uppermost Jurassic to Lower Cretaceous volcaniclastic strata of the Toro Formation and Upper Cretaceous arkosic assemblages of the Atascadero Formation (Page, 1972; Hall et al., 1979; Seiders, 1982; Jacobson et al., 2011). The Nacimiento tectonostratigraphic package is bounded and internally disrupted by several strands of the dextral San Andreas fault system, including Nacimiento, Santa Ynez River, San Gregorio–Hosgri, Oceanic–West Huasna, East Huasna, and Big Pine faults (Fig. 2).

Subduction assemblages in the Nacimiento block have long been considered an element of the Franciscan Complex (e.g., Bailey et al., 1964; Gilbert, 1973; Ernst, 1980; Korsch, 1982; Hall, 1991; Dickinson et al., 2005; Ducea et al., 2009; Hall and Saleeby, 2013). The Nacimiento Franciscan is a tectonic assemblage of sandstone, siltstone, shale, chert, conglomerate, serpentinite, and basaltic rocks variably metamorphosed along a HP/LT trajectory (Hsü, 1969; Gilbert, 1973; Cowan and Page, 1975; Ernst, 1980; Underwood et al., 1995; Underwood and Laughland, 2001). Three distinct types of units comprise the Nacimiento Franciscan: (1) broken formation consisting of internally sheared yet coherent well-bedded sandstone and turbidite sequences that lack exotic blocks; (2) a chaotically sheared (mélange) unit consisting mainly of clastic and greenstone blocks within a foliated siliciclastic matrix and containing <1% exotic blocks of chert, blueschist, and serpentinite; and (3) coherent unmetamorphosed submarine fan systems interpreted as trench-slope or trench-axis basin assemblages (slabs) lying in depositional contact above, and containing detritus from, the subduction complex (Hsü, 1968; Gilbert, 1973; Smith et al., 1979; Becker and Cloos, 1985; Underwood and Howell, 1987; Hall, 1991; Underwood and Laughland, 2001; Dickinson et al., 2005; Jacobson et al., 2011; Ogawa et al., 2014).

Primary sedimentary features are best preserved in feebly recrystallized strata adjacent to the Pacific Ocean and are progressively metamorphosed to an increasing degree inland. Based on mineralogy and bulk-rock compositions, Ernst (1980) classified the Nacimiento Franciscan into three metamorphic

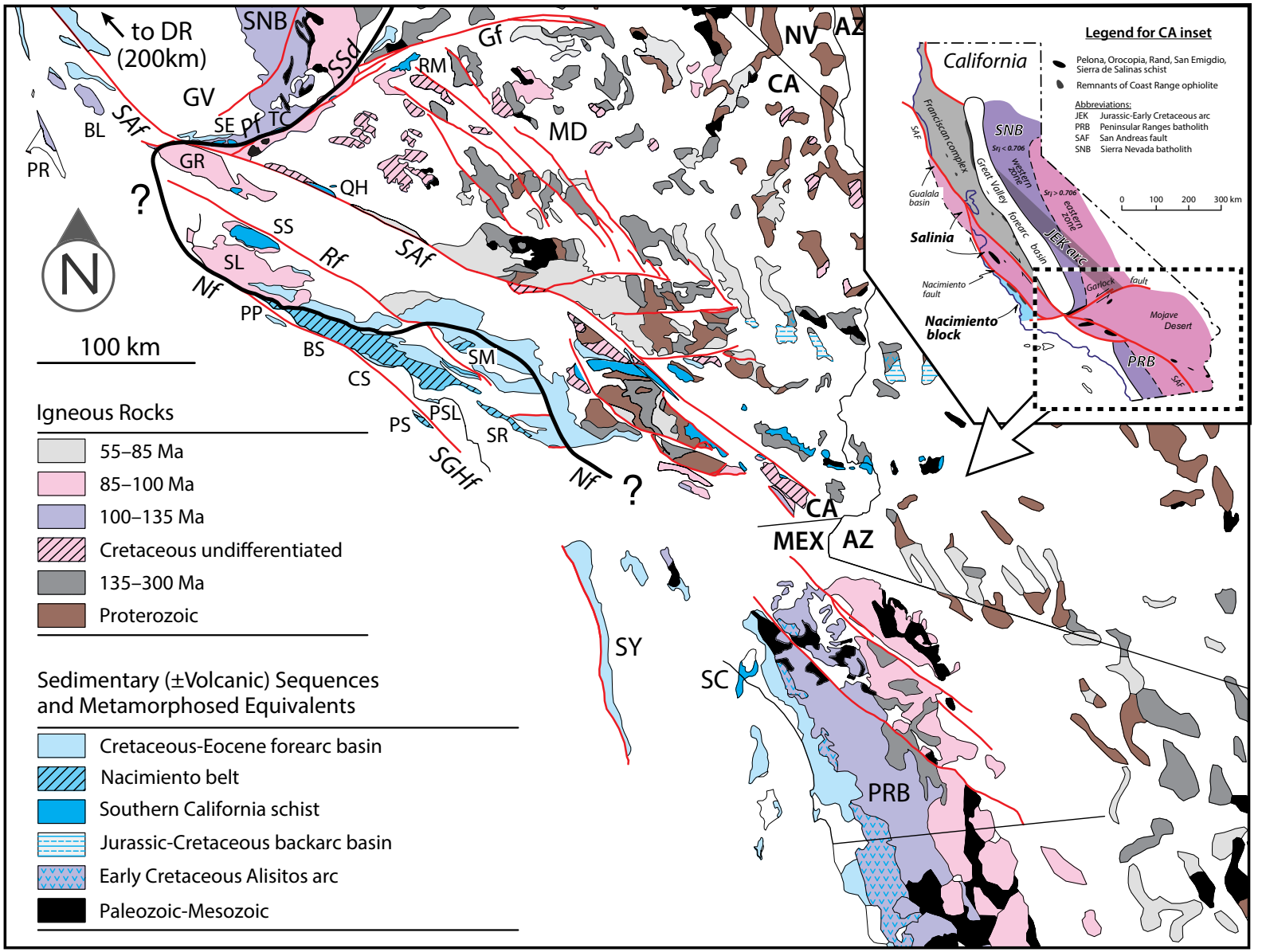

Figure 1. Pre–San Andreas palinspastic reconstruction of southern California, SW Arizona, and NW Mexico after Grove et al. (2003) and Jacobson et al. (2011). Inset after Chapman et al. (2012). Location of Jurassic–Early Cretaceous (JEK) arc from Saleeby and Dunne (2015). Abbreviations: BL—Ben Lomond Mountain; BS—Big Sur; CS—Cambria Slab; DR—Diablo Range; GR—Gabilan Range; GV—Great Valley; MD—Mojave Desert; PP—Pigeon Point; PR—Point Reyes; PRB—Peninsular Ranges batholith; PS—Point Sur; PSL—Point San Luis Slab; QH—Quartz Hill; RM—Rand Mountains; SC—Santa Catalina Island; SE—San Emigdio Mountains; SL—Santa Lucia Mountains; SM—Stanley Mountain window; SNB—Sierra Nevada batholith; SR—San Rafael Mountains; SS—Sierra de Salinas; SY—Santa Ynez Mountains; TC—Tehachapi Mountains. Fault abbreviations: Gf—Garlock; Nf—Nacimiento; Pf—Pastoria fault; Rf—Reliz-Rinconada; SAf—San Andreas; SGHf—San Gregorio–Hosgri; SSd—Southern Sierra detachment.

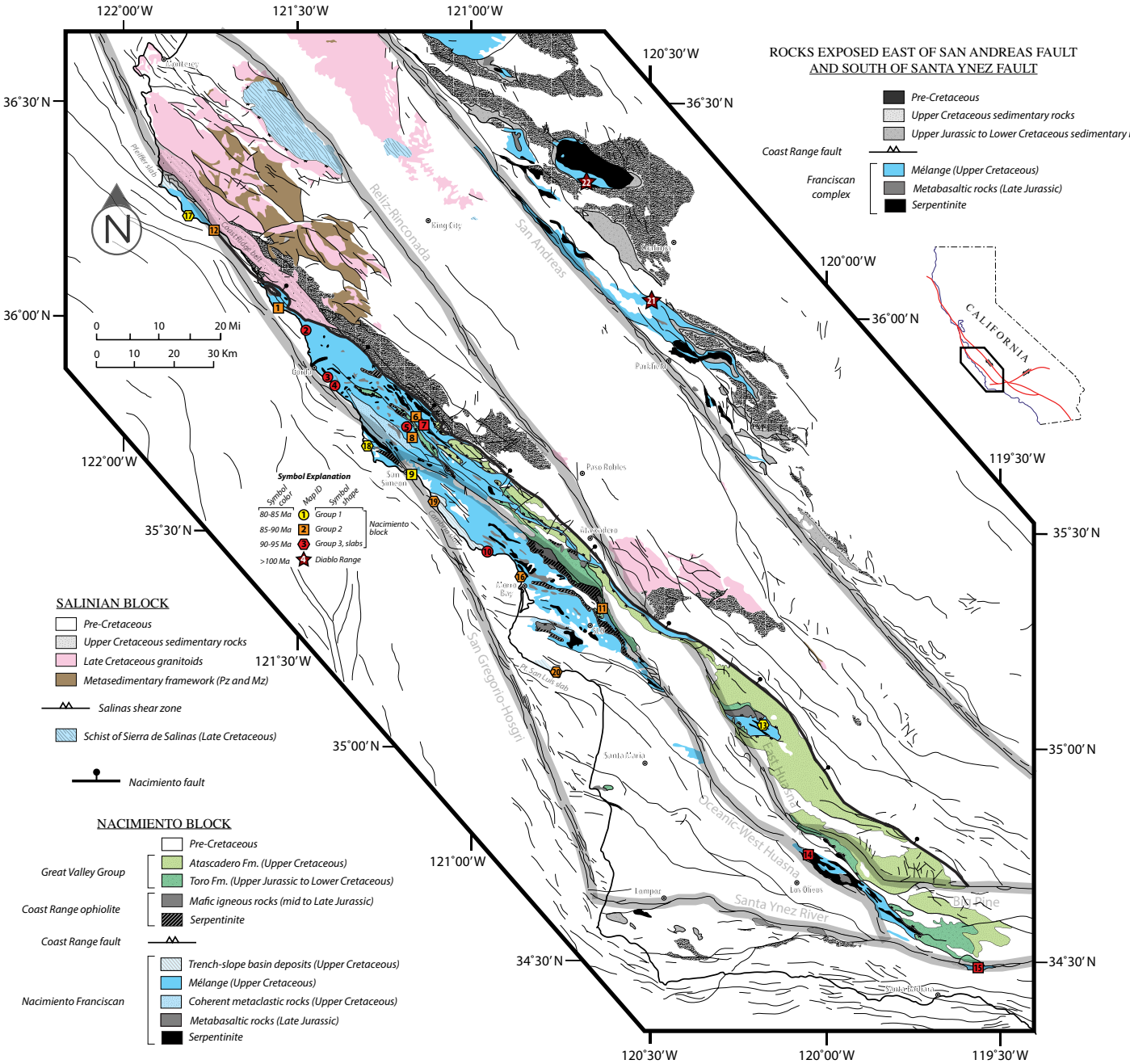

Figure 2. Geologic map of the Nacimiento block and adjacent areas. Locations of clastic rocks sampled for detrital zircon geochronology shown as circles (Group 1), squares (Group 2), hexagons (Group 3 and Type E), and stars (Diablo Range Franciscan). Field sample identifiers, coordinates, map units, rock types and inferred protoliths, metamorphic grades, sample groups, and calculated maximum depositional ages in Table 1. Major fault zones outlined in broad transparent gray lines. Abbreviations: Mz—Mesozoic; Pz—Paleozoic.

zones from west to east: zone I—lacking neoblastic Ca-Al hydrous silicates; zone II—pumpellyite bearing; and zone III—lawsonite ± jadeitic pyroxene bearing. The Nacimiento section is interpreted to have undergone recrystallization during subduction under temperatures of ~150–300 °C at lithostatic pressures ranging from 2 to 3 kbar in the west to 5–8 kbar in the east (Ernst, 1980) and may also have been affected by an episode of postsubduction heating (Underwood et al., 1995; Underwood and Laughland, 2001).

Assembly, mélange formation, and exhumation of the Nacimiento Franciscan are thought to have occurred by some combination of progressive accretion and underplating; tectonic, sedimentary, and diapiric mixing; and extension plus return flow within the accretionary wedge (e.g., Hsü, 1968; Cloos, 1982; Platt, 1986, 2015). Blueschist-facies metamorphism of mafic blocks in mélange near San Simeon at ca. 155–150 Ma is thought to constrain the onset of subduction in the Nacimiento block (Ukar, 2012; Ukar et al., 2012). Paleontological, K-Ar whole-rock, ^{40}Ar-^{39}Ar detrital K-feldspar, and U-Pb detrital zircon ages ranging between ca. 90 and 70 Ma suggest that significant delivery and accretion of clastic detritus to the trench did not take place until >60 m.y. later (Hsü, 1969; Gilbert, 1971; Page, 1972; Suppe and Armstrong, 1972; Gilbert, 1973; Seiders, 1983; Underwood et al., 1995; Jacobson et al., 2011).

Franciscan Complex

The "type" Franciscan Complex crops out east of the Salinian block and consists of three fault-bounded belts decreasing in depositional age of clastic materials structurally downward: the Eastern, Central mélange, and Coastal belts (Bailey et al., 1964; Berkland et al., 1972; Blake et al., 1988; Jayko et al., 1989; McLaughlin et al., 1994, 2000; Dumitru et al., 2015; Wakabayashi, 2015). The Nacimiento Franciscan is most similar to the Central belt, both of which contain abundant mélange, but chaotic units also are present in the other Franciscan belts (Cowan, 1978; Raymond, 1984, 2015; Aalto, 2014; Wakabayashi, 2015).

According to the sinistral slip model for the Nacimiento fault, the Nacimiento Franciscan was emplaced outboard of eastern and/or central Franciscan belt rocks of the Diablo Range and San Francisco Bay Area (Jacobson et al., 2011). A stack of broadly folded and downward-younging thrust sheets, comprising chiefly blueschist and lawsonite-albite facies Franciscan coherent and mélange units, crops out in the core of the Diablo Range (Ernst, 1993; Ernst et al., 2009; Snow et al., 2010; Wakabayashi, 2015). This structure is disrupted by multiple strands of the San Andreas fault in the southern Diablo Range, resulting in several exposures of Franciscan rocks in the cores of NW-trending open folds near Coalinga and Parkfield (e.g, Irwin and Barnes, 1975; Fig. 2).

High-pressure/low-temperature mineral assemblages and thrust structures preserved in the Diablo Range and in Franciscan assemblages in northern California are widely regarded to reflect progressive underplating and metamorphism attending subduction of the oceanic Farallon plate beneath North America from Middle to Late Cretaceous time (Ernst, 1970, 1993; Mattinson and Echeverria, 1980; Unruh et al., 2007; Ernst et al., 2009; Snow et al., 2010; Dumitru et al., 2010, 2015; Wakabayashi, 2015).

Rand-Type Schists

The Rand, San Emigdio, and Sierra de Salinas schists (referred to in aggregate as "the Rand-type schist") and similar early Cenozoic Pelona and Orocopia schists of more southerly California crop out along detachment structures beneath older crystalline rocks of the SW Cordilleran batholithic belt (Graham and England, 1976; Haxel and Dillon, 1978; Ehlig, 1981; Jacobson, 1983, 1995; Jacobson et al., 1988, 2007, 2011; Simpson, 1990; Kidder and Ducea, 2006; Ducea et al., 2009; Chapman et al., 2010, 2011, 2012). Most workers agree that deposition and emplacement of the schist occurred during an episode of shallow subduction (see footnote 1) related to the Laramide orogeny (Jacobson et al., 2007 and references therein).

The deposition, subduction, and early phases of structural ascent of the schist are temporally and spatially associated in plate reconstructions with the subduction of an oceanic plateau (Saleeby, 2003; Liu et al., 2008, 2010). Plateau subduction beneath the southernmost Sierra Nevada batholith and adjacent southern California batholith is hypothesized to have driven slab flattening, leading to the tectonic removal of sub-batholithic mantle lithosphere, cessation of arc magmatism, abrupt crustal thickening in the overriding batholithic plate (Malin et al., 1995; Ducea and Saleeby, 1998; House et al., 2001; Saleeby, 2003; Nadin and Saleeby, 2008) and decompression of batholithic assemblages from deep- to mid-crustal levels (Saleeby et al., 2007; Chapman et al., 2010). The resulting high-elevation mountain belt shed detritus into the trench, which was immediately underthrust beneath the recently extinguished arc and subjected to amphibolite-facies metamorphism to become the schist (Kidder and Ducea, 2006).

Sierra Nevada–Peninsular Ranges Batholith

The Cretaceous Sierra Nevada–Peninsular Ranges arc is a NNW-trending composite batholith, constructed from ca. 140–80 Ma (e.g., Chen and Moore, 1982; Chapman et al., 2012; Kimbrough et al., 2014; Nadin et al., 2016). Pluton ages, bulk compositions, amounts of recycled crustal components, and the paleogeographic affinities of metamorphic wall rocks define a distinct west-to-east zonation (Fig. 1). For example, the western arc generally contains ca. 140–100 Ma tonalitic and gabbroic plutons emplaced into Paleozoic to Mesozoic deep-water (slope and abyssal) strata and ophiolitic crust (Chapman et al., 2012 and references therein). In contrast, ca. 100–80 Ma granodioritic and granitic plutons invade a framework of mainly Paleozoic shallow-water (inner and outer shelf) passive margin strata in the eastern arc. The Cretaceous arc was emplaced across a NW-trending Jurassic–Early Cretaceous arc, and as a

result, the older arc resides outboard of the younger in central California, and vice versa in southern California (Jacobson et al., 2011; Sharman et al., 2015). The southern segment of the Cretaceous arc is referred to here as the southern California batholith (Saleeby, 2003). These spatial variations in the Sierra Nevada–Peninsular Ranges arc and its framework are useful for pinpointing the source area(s) of arc-derived detritus.

METHODS

Zircon grains were extracted from samples of subduction assemblages in the Nacimiento block (20), Franciscan rocks of the southern Diablo Range (2), and Rand-type schists of the Mojave Desert (2) (Table 1) using standard mineral separation techniques of crushing, sieving, magnetic separation, processing through heavy liquids, and handpicking. Separates were then mounted in epoxy, polished, and imaged on scanning electron microscope systems at Stanford University and Missouri University of Science and Technology (S&T) prior to analysis. Twenty samples (Fig. 2; Table 1) were analyzed by laser-ablation–multicollector–inductively coupled plasma–mass spectrometry (LA-MC-ICP-MS) at the Arizona LaserChron Center (ALC) following methods outlined in Gehrels et al. (2006). Zircon grains were ablated using a 193 nm ArF laser with a pit depth of ~12 μm and spot diameters of 25–30 μm, depending on grain size. Fragments of an in-house Sri Lanka (SL) zircon standard with an isotope dilution–thermal ionization mass spectrometry (ID-TIMS) age of 563.5 ± 3.2 Ma (2σ) were analyzed once per every five unknown analyses to correct for instrument mass fractionation and drift (Gehrels et al., 2008). A secondary standard R33 (Black et al., 2004) with ID-TIMS age of 418.9 ± 0.4 Ma (2σ) was analyzed once per every 50 unknown analyses, permitting comparison of ALC results with data from the University of California–Santa Cruz (UC Santa Cruz) laboratory. Data reduction was done using in-house ALC Microsoft Excel programs and Isoplot/Ex, version 3 (Ludwig, 2003).

Zircon grains from the remaining four samples (Fig. 2; Table 1) were hand selected from concentrates, mounted together with primary R33 (Black et al., 2004) and secondary standard AS3/FC3 (Schmitz et al., 2003), imaged by optical and scanning electron microscopy at Stanford, and analyzed at UC Santa Cruz using a Photon Machines Analyte 193 excimer laser coupled with a single

TABLE 1. SUMMARY OF FIELD, PETROGRAPHIC, AND GEOCHRONOLOGIC DATA

Figure 2 ID	Field ID	Location	Block	Sub-block[a]	UTM zone[b]	UTM Easting[b]	UTM Northing[b]	Depth below Nacimiento fault (km)[c]	Depth below Coast Range fault (km)[c]
1	11SL1	N. Santa Lucia Range	Nacimiento	3	10S	629784	3987317	2	ND
2	11SL2	N. Santa Lucia Range	Nacimiento	3	10S	635943	3983176	1	ND
3	10NB2	N. Santa Lucia Range	Nacimiento	3	10S	642864	3969434	8	6
4	10NB1	N. Santa Lucia Range	Nacimiento	3	10S	644021	3967956	9	5
5	SLO-387*	S. Santa Lucia Range	Nacimiento	3	10S	663266	3957080	5	2
6	SLO-401*	S. Santa Lucia Range	Nacimiento	3	10S	664410	3959034	3	0
7	SLO-402*	S. Santa Lucia Range	Nacimiento	3	10S	666010	3957662	3	0
8	SLO-382*	S. Santa Lucia Range	Nacimiento	3	10S	665484	3953005	5	2
9	11MB6	S. Santa Lucia Range	Nacimiento	2	10S	665317	3945492	10	5
10	11MB4A	S. Santa Lucia Range	Nacimiento	2	10S	685368	3925367	14	8
16	11MB3	S. Santa Lucia Range	Nacimiento	2	10S	693282	3920170	12	5
11	SLO-107*	S. Santa Lucia Range	Nacimiento	2	10S	715176	3909554	4	1
17	10NB6	N. Santa Lucia Range	Nacimiento	1	10S	606296	4011121	2	ND
12	12SL1	N. Santa Lucia Range	Nacimiento	1	10S	612487	4008060	0	ND
13	11SM1†	Stanley Mountain window	Nacimiento	4	10S	756869	3882266	5	1
18	13NB1	S. Santa Lucia Range	Nacimiento	1	10S	654613	3951239	13	1
14	13SR2	San Rafael Mountains	Nacimiento	3	10S	770185	3848498	14	1
15	LP19	Santa Ynez Mountains	Nacimiento	3	11S	264023	3818596	ND	ND
19	11MB5†	Cambria Slab	Nacimiento	2	10S	671162	3937841	10	6
20	15NB1	Pt. San Luis Slab	Nacimiento	2	10S	703902	3893095	20	7
21	13DR1	S. Diablo Range	Diablo Range	5	10S	727405	3990715	NA	NA
22	13DR3	S. Diablo Range	Diablo Range	5	10S	709609	4020979	NA	NA
NA	08QH1	Quartz Hill	Mojave	6	11S	389202	3834550	NA	NA
NA	08TC37	Tehachapi Mountains	Mojave	6	11S	366051	3873180	NA	NA

(*continued*)

TABLE 1. SUMMARY OF FIELD, PETROGRAPHIC, AND GEOCHRONOLOGIC DATA (*continued*)

Figure 2 ID	Map unit[d]	Sample	Protolith	Metamorphic Grade[e]	Analysis[f]	Nacimiento Group	Maximum Depositional Age (Ma)	2σ uncertainty (Ma)
1	KJf (gw and bs; Hall, 1991)	Mélange block	Sandstone	PP	UA	2B	86.6	2.0
2	KJf (Hall, 1991)	Broken Formation	Turbidite	Z	UA	1B	94.1	0.9
3	fs (Dibblee, 2007)	Broken Formation	Turbidite	Z	UA	1B	90.1	2.5
4	fs (Dibblee, 2007)	Broken Formation	Sandstone	Z	UA	1B	91.1	5.5
5	KJfm (Hall et al., 1979)	Mélange block	Sandstone	PP	UA	1A	98.1	1.2
6	KJfm (Hall et al., 1979)	Mélange block	Sandstone	LJ	UA	2B	85.6	2.2
7	KJfm (Hall et al., 1979)	Mélange block	Sandstone	LJ	UA	2A	92.8	2.5
8	KJfm (Hall et al., 1979)	Mélange block	Sandstone	PP	UA	2A	90.0	16.0
9	KJfm (Hall et al., 1979)	Mélange block	Sandstone	Z	UA	2B	84.6	4.3
10	KJfm (Hall et al., 1979)	Mélange block	Sandstone	Z	UA	1A	95.0	2.3
16	Ks (Hall et al., 1979)	Mélange block	Sandstone	Z	UA	3	86.0	7.3
11	KJfm (Hall et al., 1979)	Mélange block	Sandstone	LJ	UA	2B	85.5	3.7
17	KJf (Hall, 1991); KJfgw (Wills, 2001), Ks (this study)	Bedded unit encased in mélange	Sandstone	Z	UA	3	82.7	5.9
12	KJf (Hall, 1991)	Mélange block	Sandstone	Z	UA	2A	89.8	1.7
13	“diamictite” (Korsch, 1982)	Mélange block	Sandstone	LJ	UA	E	84.4	2.1
18	Ks (Hall et al., 1979)	Bedded unit encased in mélange	Turbidite	Z	UCSC	3	81.7	5.5
14	KJfm (Hall, 1981)	Mélange block	Sandstone	Z	UCSC	2A	92.8	5.5
15	fs (Dibblee, 1966)	Mélange block	Sandstone	Z	UA	2A	91.1	3.0
19	Ks (Hall et al., 1979)	Bedded unit	Sandstone	Z	UA	E	90.1	2.7
20	Ks (Hall et al., 1979)	Bedded unit	Turbidite	Z	UA	3	87.3	2.9
21	f (Dibblee, 1971)	Mélange block	Sandstone	Z	UCSC	N/A	106.3	6.4
22	fs (Dibblee, 1971)	Mélange block	Sandstone	PP	UCSC	N/A	100.1	6.0
NA	Mzpos (Hernandez, 2010)	Foliated quartzofeldspathic schist	Sandstone	A	UA	N/A	80.7	7.7
NA	qfm (Sharry, 1981)	Foliated quartzofeldspathic schist	Sandstone	A	UA	N/A	89.3	2.0

*Location approximate.
†Sample from Dumitru et al. (2016).
[a]Sub-block definitions: 1—west of San Gregorio–Hosgri fault; 2—between San Gregorio–Hosgri and Oceanic-West Huasna faults; 3—between Oceanic-West Huasna and Reliz-Rinconada–East Huasna faults; 4—between East Huasna and San Andreas faults; 5—Central California, east of San Andreas fault; 6—Southern California, east of San Andreas fault.
[b]Universal Transverse Mercator (UTM) coordinates are World Geodetic System 1984 datum.
[c]Depths estimated based on regional attitudes of foliation and map view distances to Nacimiento and Coast Range faults. ND—not determined.
[d]Map unit abbreviations: bs—blueschist; f—Franciscan shale, graywacke, chert, jasper, glaucophane rock, mixed and sheared; fs—graywacke sandstone and minor dark gray shale; gw—graywacke; KJf—Cretaceous-Jurassic Franciscan undifferentiated; KJfgw—Cretaceous-Jurassic Franciscan graywacke; KJfm—Cretaceous-Jurassic Franciscan mélange; Ks—Cretaceous unnamed sandstone; Mzpos—Mesozoic Portal schist; qfm—”Pelona” quartz-feldspar-muscovite schist.
[e]Metamorphic grade: Z—zeolite and lower (zone 1 of Ernst, 1980); PP—prehnite-pumpellyite (zone 2 of Ernst, 1980); LJ—lawsonite- and/or jadeitic pyroxene-bearing (zone 3 of Ernst, 1980); A—amphibolite.
[f]Location of U-Pb detrital zircon analysis; UA—University of Arizona; UCSC—University of California, Santa Cruz.

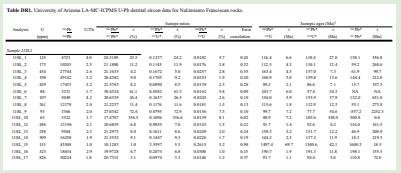

collector Thermo Element XR magnetic sector ICP-MS. Data reduction and age calculations were performed using Iolite software (Paton et al., 2011). Isotopic data and analytical uncertainties are provided for ALC- and UC Santa Cruz–based analyses in Tables SD1 and SD2 in the Supplemental File[2].

Normalized and cumulative probability plots comparing analyzed samples were constructed with ALC Microsoft Excel programs using $^{207}Pb/^{206}Pb$ ages for grains older than 800 Ma and $^{206}Pb/^{238}U$ ages for grains younger than 800 Ma. Analyses with greater than 10% uncertainty, 30% discordance, and/or 5% reverse discordance were excluded. Maximum depositional ages were calculated for each sample from weighted averages of the three youngest detrital grains (e.g., Dickinson and Gehrels, 2009). Detrital zircon geochronologic data generated in this effort were not integrated with those of Morisani (2006) from San Simeon due to concerns therein regarding data reproducibility.

Multidimensional scaling (MDS) is a technique that allows visualization of statistical dissimilarities between arrays of data on a two-dimensional “map.” The technique has recently been applied to arrays of detrital zircon age data to produce MDS maps on which statistically similar samples plot close together and dissimilar samples plot farther apart (Vermeesch, 2013). The utility of MDS mapping lies in the ability to visualize similar and dissimilar arrays of detrital zircon data from a large number of samples in a much quicker and less

[2]Supplemental File. Analytical techniques, petrographic data, ICP-MS zircon U-Pb datasets, and cathodoluminescence images of zircon mineral separates. Please visit http://dx.doi.org/10.1130/GES01257.S1 or the full-text article on www.gsapubs.org to view the Supplemental File.

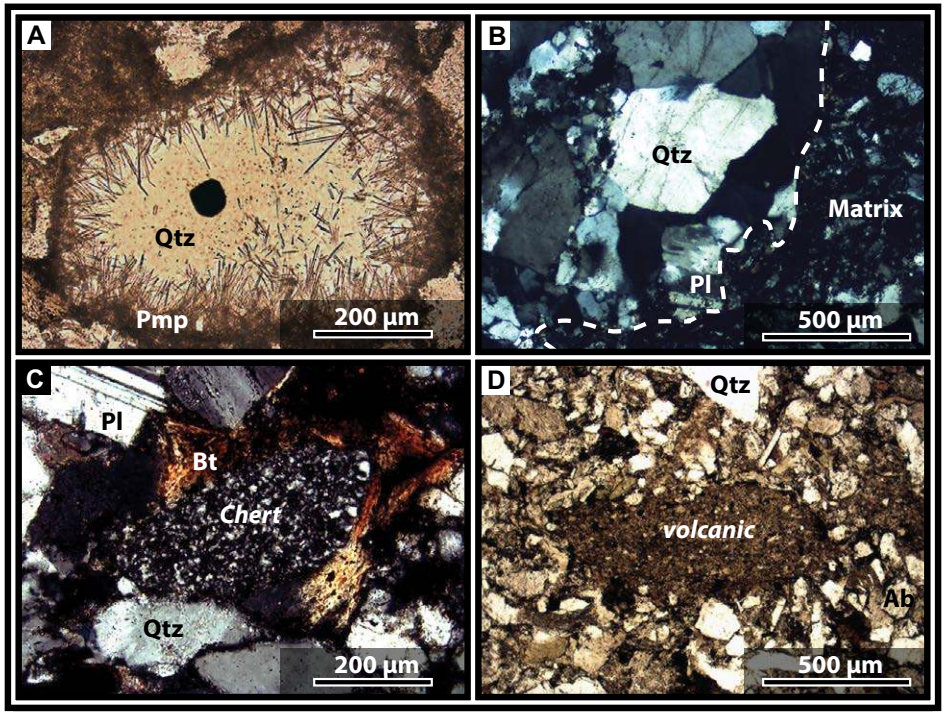

Figure 3. Photomicrographs of petrologic features in Nacimiento Franciscan (meta) sandstones. (A) Sample 11SM1—Needles of pumpellyite in detrital quartz grain. Opaque grain is iron oxide; plane polarized light (ppl). (B) Sample 11SL1—Tonalite clast in fine siliciclastic matrix; cross polarized light (xpl). (C) Sample 10NB6—Chert lithic fragment in sandstone; xpl. (D) 11MB6—Felsic volcanic fragment in sandstone. Mineral abbreviations: Bt—biotite; Pl—plagioclase; Pmp—pumpellyite; Qtz—quartz.

cumbersome manner than visually comparing numerous probability density curves. The MDS mapping algorithm (Chapman et al., 2012, 2015; Vermeesch, 2013) used here to compare U-Pb detrital zircon spectra is as follows: (1) Input square, symmetric matrix of Kolmogorov-Smirnov (K-S) distances between samples; (2) assign points to arbitrary coordinates in two-dimensional (2-D) space; (3) compute K-S distances among all pairs of points, to form a new matrix; (4) compare the new matrix with the input matrix by evaluating the stress function, a measure of the degree of correspondence between the observed and reproduced distances; (5) perturb the coordinates of each data point; and (6) repeat steps 2 through 5 until stress is minimized.

RESULTS

Sandstone Petrography

Petrographic results are tabulated in the Supplemental File. All Nacimiento Franciscan samples contain recognizable detrital mineral grains, lithic fragments, and carbonaceous matter moderately to significantly overprinted by secondary metamorphic parageneses (Fig. 3). Detrital grains of quartz and plagioclase comprise 37–70 modal percent of these rocks, in approximately subequal proportions (Fig. 4). Other phases, comprising up to 13 modal percent, include nearly ubiquitous clastic grains of epidote, white mica, chlorite, biotite, titanite, opaques, Ca-carbonates, and organic matter. Trace detrital grains include K-feldspar, clinopyroxene, garnet, tourmaline, apatite, and zircon. Neoblastic minerals include white mica flakes (replacing irresolvable clays), stilpnomelane (after biotite), and zeolites + pumpellyite + lawsonite (replacing the anorthite component of plagioclase). Five categories of lithic fragments were distinguished, including shale, siltstone, chert, dacitic-to-rhyolitic volcanic debris, and tonalitic plutonic clasts (Fig. 3). In aggregate, rock fragments comprise from 4 to 41 modal percent of the studied metasandstones. Proportions of all lithic clast types decrease eastward with increasing metamorphic grade. K-feldspar is absent from most studied samples but is present in small quantities (<3 modal percent) in a few weakly altered zone I Nacimiento Franciscan and trench-slope basin deposits. Biotite is rare and epidote is absent from the most intensely recrystallized, lawsonite-bearing zone III metasandstones. Franciscan metaclastic assemblages of the Nacimiento block plot mainly within the “dissected arc” but extend slightly into “transitional arc” and “basement uplift” fields on a QFL ternary diagram (Dickinson and Suczek, 1979; Fig. 4).

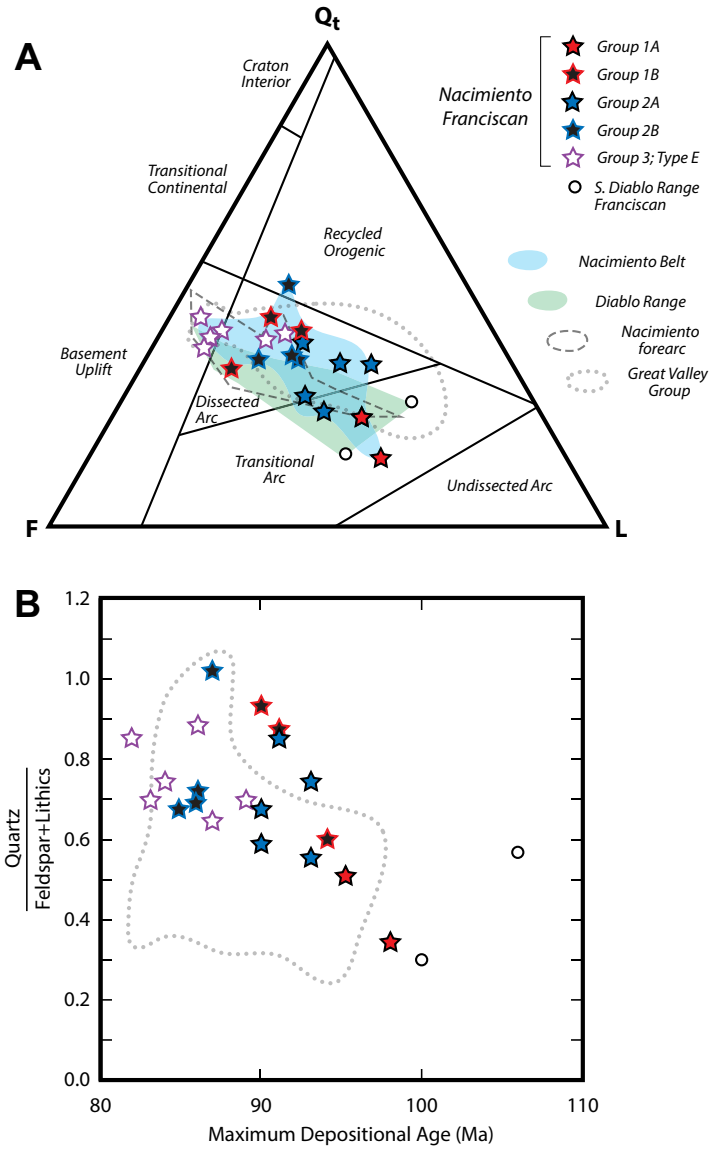

Figure 4. (A) QFL diagram showing range in detrital modes of Nacimiento and Diablo Range Franciscan rocks compared to published data from the Nacimiento Franciscan (Gilbert, 1973; Lee-Wong and Howell, 1977; Smith, 1978; Ernst, 1980; Dickinson et al., 1982), Diablo Range Franciscan (Cowan, 1974; Jacobson, 1978), Atascadero Formation ("Nacimiento Forearc"; Gilbert and Dickinson, 1970; Mackinnon, 1978; Jacobson et al., 2011), and Great Valley Group (Mansfield, 1979; Ingersoll, 1978, 1983). (B) Plot of maximum depositional age versus compositional maturity index. Note increasing compositional maturity in Nacimiento Franciscan lithologies with time.

Detrital Zircon Geochronology

Samples of Nacimiento Franciscan rocks yielded a total of 1735 zircon analyses suitable for provenance analysis (i.e., analyses with less than 10% uncertainty, 30% discordance, and/or 5% reverse discordance; Tables SD1 and SD2 in the Supplemental File). Normalized and cumulative probability plots of detrital zircon ages from both suites are presented in Figures 5 and 6. Maximum depositional ages calculated from the Nacimiento Franciscan do not appear to vary along strike, perpendicular to strike, or with structural depth below the Coast Range fault or Nacimiento fault (Fig. 2; Table 1).

Four distinct groups of clastic rocks are apparent based on detrital zircon age distributions and calculated maximum depositional ages (Figs. 4, 5, and 6). Of these, Group 1 assemblages yield the oldest maximum depositional ages, ranging from 90.1 ± 2.5 Ma (2σ, mean square of weighted deviates [MSWD] = 0.102) to 98.1 ± 1.2 Ma (2σ, MSWD = 0.033). These samples share a major age peak centered at ca. 100 Ma, with 75% of all grains falling between 120 and 80 Ma, one-quarter of which are Late Cretaceous (<100 Ma). Jurassic to earliest Cretaceous (200–120 Ma) grains comprise the majority of remaining Group 1 grains (19% of the total) with minor (5%) proportions of Triassic, Paleozoic, and Precambrian grains. Additional subdivision of Group 1 rocks is possible based on maximum depositional ages and lithologic relations. Group 1A rocks were collected from blocks of sub-zeolite to prehnite-pumpellyite facies metasandstone in dull gray shale mélange also including abundant chert, greenstone, and rare blueschist blocks (Fig. 7). These metasandstones exhibit the oldest maximum depositional ages (ca. 98–95 Ma) of samples studied here and contain the highest proportions of lithic fragments (~40% by mode), dominated by volcanic and chert debris. Group 1B samples are from exposures of broken formation (Hsü, 1968; Fig. 7) turbidite sequences characterized by alternating fine-grained sandstone and siltstone intervals traceable over distances of ~1–10 m, the presence of cross-cutting intermediate dikes ~10 cm to 1 m wide (Fig. 7B), and a lack of exotic blocks. A single turbidite block ~3 km south of Gorda is mappable along State Highway 1 for more than four kilometers and is encased in a fine siliciclastic matrix (Fig. 7). In comparison with Group 1A, these rocks yield younger maximum depositional ages (ca. 94–90 Ma), contain higher proportions of detrital quartz grains (~26%–33%), appear to lack volcanic fragments, and show no evidence for metamorphic recrystallization. Both Group 1 subgroups are geographically restricted to a relatively outboard position in the Nacimiento block within ~50 km of San Simeon.

A second group of Franciscan rocks, collected from metasandstone blocks in mélange (Fig. 7), appears to be distributed throughout the entire length and width of the Nacimiento block. Group 2 rocks yield younger maximum depositional ages than those of Group 1, ranging from 84.6 ± 4.3 Ma (2σ, MSWD = 0.16) to 92.8 ± 2.5 Ma (2σ, MSWD = 0.054). Compared to Group 1, Group 2 metasandstones contain significantly higher proportions of Jurassic to earliest Cretaceous (48%) and smaller populations of 120–80 Ma (42%) grains. Two-thirds of this latter population of grains are Late Cretaceous in age. Like Group 1, Group 2 rocks contain small amounts (6%) of Triassic and older grains.

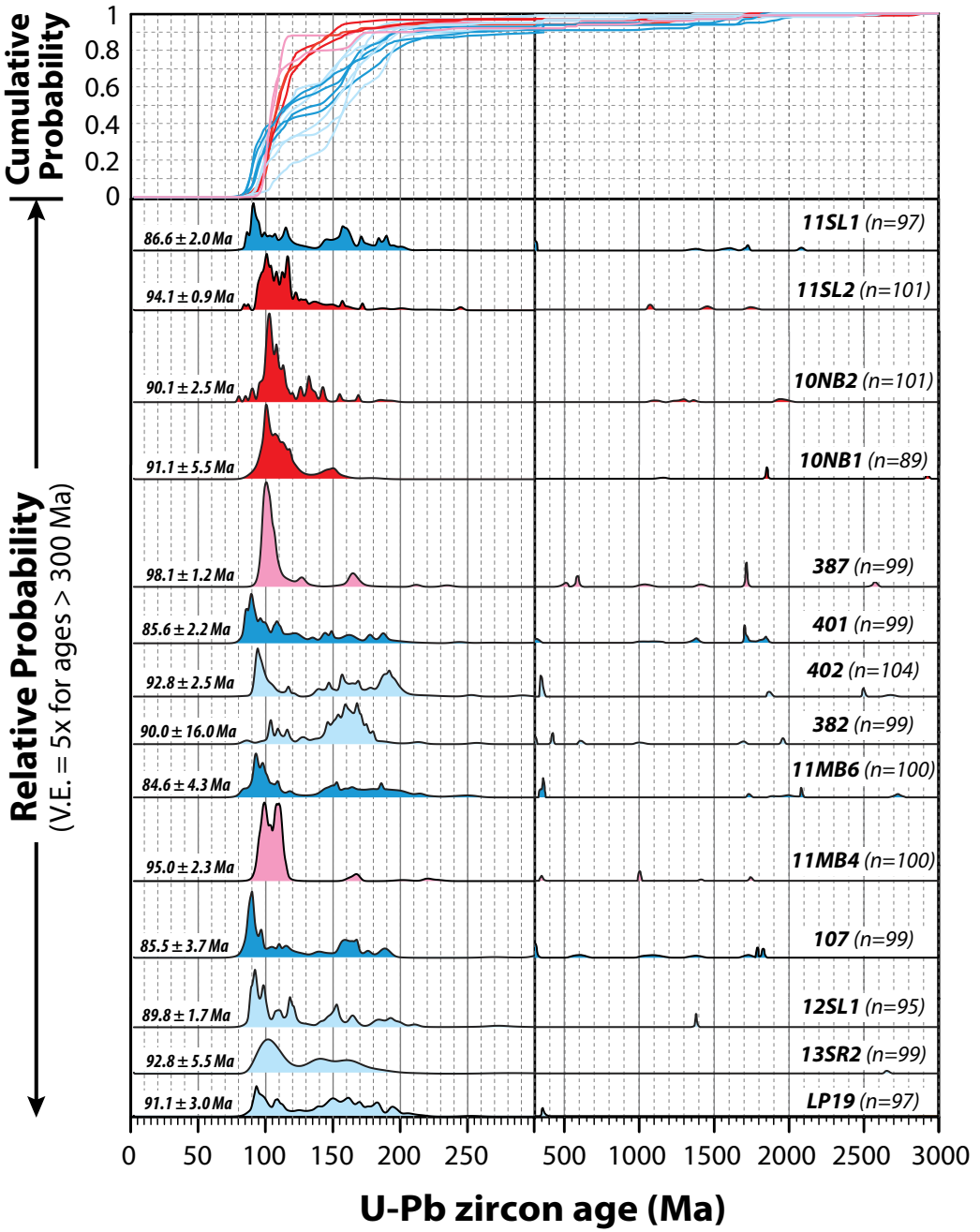

Figure 5. Normalized and cumulative probability plots comparing zircon ages from Group 1A (pink), 1B (red), 2A (light blue), and 2B (blue) Nacimiento Franciscan samples, showing the number (n) of grains analyzed. Samples arranged from north (top) to south (bottom) according to restored positions in Figure 1. Note the split horizontal axis at 300 Ma and that spectra between 300 and 3000 Ma are vertically exaggerated by a factor of five. Maximum depositional ages calculated as a weighted mean of the three youngest grains that overlap in analytical error. Isotopic data in Tables SD1 and SD2 in the Supplemental File.

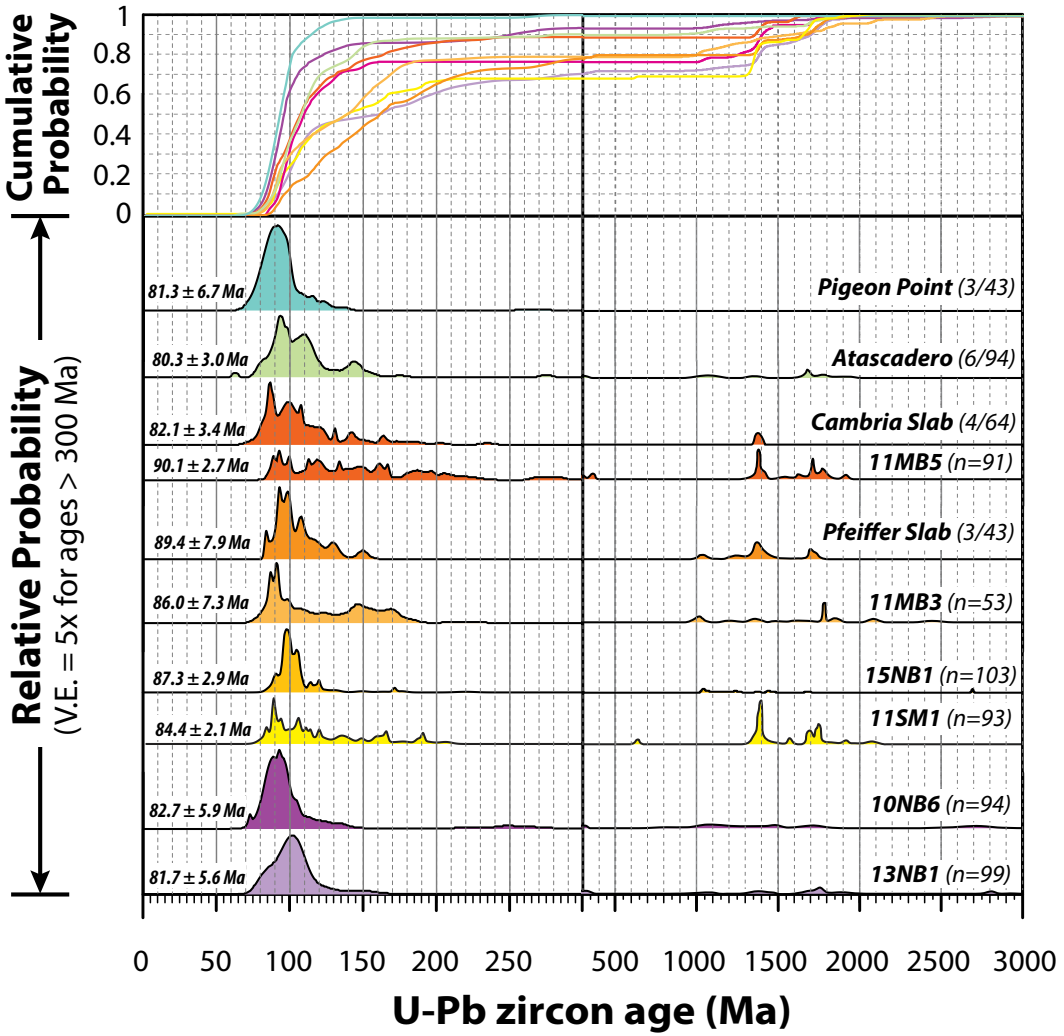

Figure 6. Normalized and cumulative probability plots comparing zircon ages from Nacimiento Group 3 (purple hues), slabs (orange to yellow), and forearc basin (green hues) deposits, showing the number of samples/grains (e.g., 3/43) analyzed. Data from Jacobson et al. (2011) and this study. Note the split horizontal axis at 300 Ma and that spectra between 300 and 3000 Ma are vertically exaggerated by a factor of five. Maximum depositional ages calculated as a weighted mean of the three youngest grains that overlap in analytical error. Isotopic data in Tables SD1 and SD2 in the Supplemental File.

Group 2 is also divisible into two subgroups. Group 2A samples yield maximum depositional ages of ca. 93–90 Ma and have lithic contents of 14%–23% (the majority of which are sedimentary). Group 2B samples, in contrast, have maximum depositional ages of 87–84 Ma and lithic fragment contents of 20%–34% (most of which are volcanic). Sample LP19, a metasandstone collected north of Santa Barbara along the Santa Ynez fault (i.e., at the southern boundary of the Nacimiento block) exhibits detrital zircon ages and petrographic features similar to those of Nacimiento Group 2A. Compared to Group 1, Group 2 rocks are more recrystallized, with the majority of Group 2 rocks containing neoblastic prehnite, pumpelleyite, lawsonite, and/or jadeitic pyroxene.

A third group of clastic rocks mapped as blocks of interbedded sandstone and siltstone within the Franciscan Complex (Hall et al., 1979; Hall, 1991) exhibits detrital zircon ages distinct from those of the previously discussed groups. This group yields maximum depositional ages ranging from 81.7 ± 5.5 Ma (2σ, MSWD = 0.25) to 87.3 ± 2.9 Ma (2σ, MSWD = 0.25). Like Group 1, Group 3 samples are dominated by grains in the 120–80 Ma age range (71%).

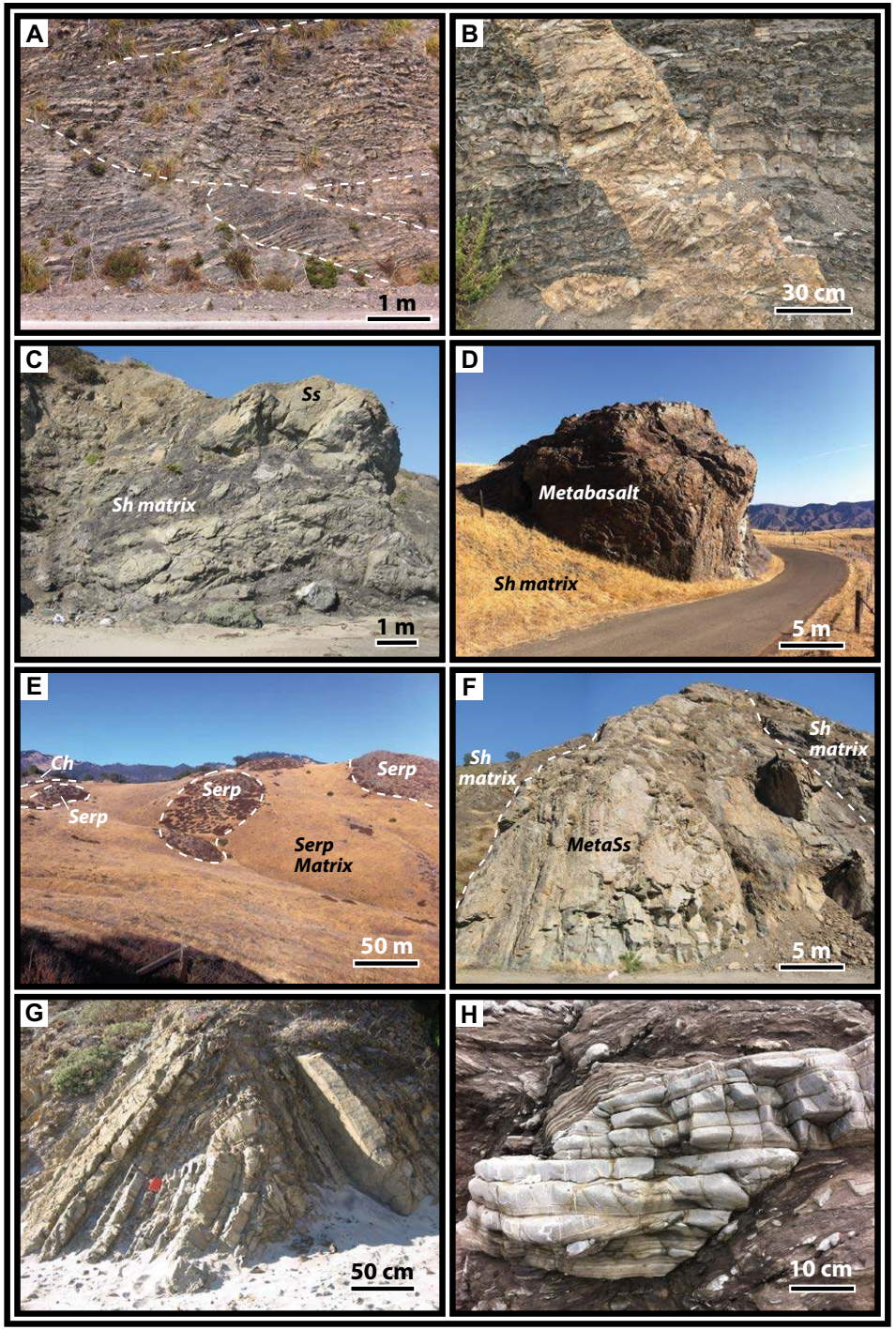

Figure 7. Field photographs of structural and petrologic features in Franciscan assemblages within and outside the Nacimiento block. (A) Nacimiento Franciscan Group 1 broken formation turbidite exposure and location of sample 11SL2 along Highway 1, Santa Lucia Range. Dashed lines show boundaries of coherent turbidite strata. (B) Nacimiento Franciscan Group 1 broken formation turbidite intruded by ~0.5-m-wide intermediate dike. Photograph taken ~1 km south of the location of sample 11SL2. (C) Nacimiento Franciscan Group 2 mélange at location of sample 11MB6 ~1 km east of San Simeon. (D) Diablo Range greenstone block in mélange at location of sample 13DR1 along Parkfield Grade. (E) Nacimiento Franciscan Group 2 mélange at location of sample 13SR2 along Figueroa Mountain Road, San Rafael Mountains. Dashed lines show block-matrix contacts. (F) Nacimiento Franciscan Group 2 metasandstone block in mélange and location of sample 11SM1 along Highway 166, Stanley Mountain window. Dashed lines show block-matrix contacts. (G) Nacimiento Franciscan folded Group 3 turbidite block in mélange (block boundaries not observed in photograph) and location of sample 10NB6 at Pfeiffer Beach. (H) Nacimiento Franciscan Group 3 turbidite block in mélange and location of sample 13NB1 ~3 km north of Piedras Blancas point. Abbreviations: Ch—chert; Serp—serpentinite; Sh—shale; Ss—sandstone.

Compared to Group 1 and Group 2, Group 3 samples contain higher proportions of Late Cretaceous (42%) and Proterozoic to Archean (13%) grains and less Jurassic to earliest Cretaceous (12%) grains. Group 3 rocks lack neoblastic minerals and contain higher quartz to feldspar plus lithic fragment ratios than Group 1 or 2 assemblages (Fig. 4).

A fourth group of samples, termed Type E by Dumitru et al. (2016), show detrital zircon age patterns characterized by a relatively few ca. 120–80 Ma grains (33%), an intermediate amount of Jurassic to earliest Cretaceous (33%) grains, and the highest proportions of Proterozoic to Archean (26%) and Triassic to Permian (7%) age grains of all groups considered. Type E samples contain two prominent age peaks at 1650–1800 Ma and 1380 Ma that are not observed in other Cretaceous sandstones from the forearc or trench. New and existing data (Jacobson et al., 2011; Dumitru et al., 2016) from Type E samples, which include unmetamorphosed Nacimiento "slabs" and a neoblastic pumpellyite- and lawsonite-bearing mélange block from the Stanley Mountain window (location 13 on Fig. 2), are compiled in Figure 6. Calculated maximum depositional ages for individual Type E samples range from 82.1 ± 3.4 Ma (2σ, MSWD = 0.26) to 90.1 ± 2.7 Ma (2σ, MSWD = 0.29) (Jacobson et al., 2011; Dumitru et al., 2016).

Figure 8 provides a comparison of our new detrital zircon geochronologic data from Nacimiento Franciscan assemblages with 177 new concordant U-Pb ages from southern Diablo Range Franciscan metasandstones, 168 new concordant U-Pb ages from Rand-Type schist exposures at Quartz Hill and in the

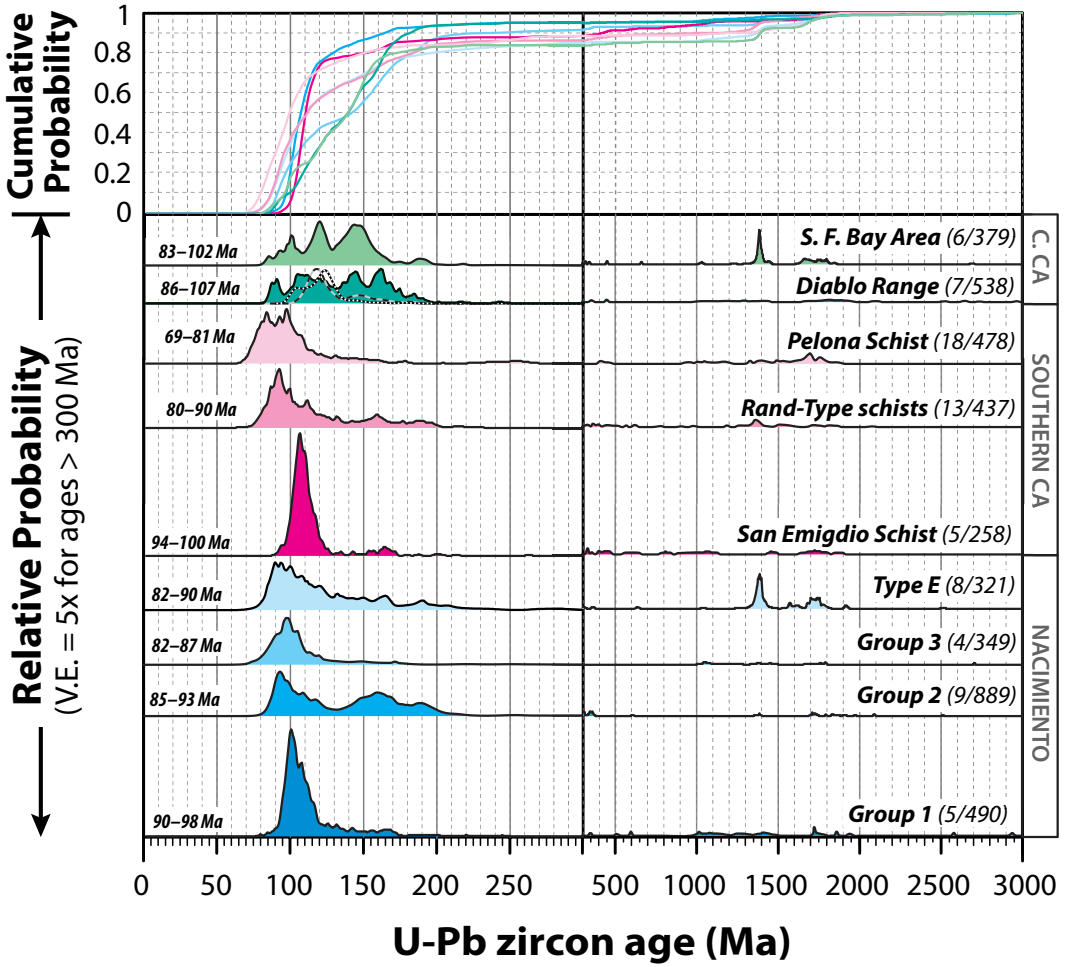

Figure 8. Normalized and cumulative probability plots comparing zircon ages from Nacimiento groups (blue hues), possibly correlative Rand-type schists (pink hues; Mojave Desert schists include exposures in the Sierra de Salinas, Rand Mountains, Tehachapi Mountains, Portal Ridge, and Quartz Hill), and possibly correlative central California Franciscan assemblages (green hues), showing the number of samples/grains analyzed. Samples 13DR1 (dashed black-gray line) and 13DR3 (white dotted line) from the southern Diablo Range are overlain on the Diablo Range aggregate curve. One sample containing detrital zircon grains as young as ca. 52 Ma (Snow et al., 2010) and two samples with youngest grains >120 Ma (Prohoroff et al., 2012), all from the San Francisco Bay Area, were not included in the interest of comparing samples with Late Cretaceous maximum depositional ages. Maximum depositional age ranges for individual samples within each group shown to left of plotted curves. Data from Barth et al. (2003), Grove et al. (2003), Unruh et al. (2007), Ernst et al. (2009), Snow et al. (2010), Jacobson et al. (2011), Prohoroff et al. (2012), Chapman et al. (2013), and this study. Note the split horizontal axis at 300 Ma and that spectra between 300 and 3000 Ma are vertically exaggerated by a factor of five. Maximum depositional ages calculated as a weighted mean of the three youngest grains that overlap in analytical error. Abbreviations: CA—California; C.—central; V.E.—vertical exaggeration.

Tehachapi Mountains, and existing data from other potential correlatives to the Nacimiento Franciscan. Southern Diablo Range Franciscan metasandstones feature prominent age peaks at ca. 120 and 144 Ma and contain a higher proportion of Jurassic–earliest Cretaceous (52%) versus 120–80 Ma (42%) grains and few (6%) Proterozoic grains. Maximum depositional ages of southern Diablo Range metasandstones are older (ca. 106–100 Ma) than those calculated from Nacimiento assemblages. Approximately half of detrital zircon grains extracted from Rand-Type schists are Middle to Late Cretaceous in age, with two-thirds of these grains yielding ages between 100 and 80 Ma. Jurassic to Early Cretaceous (120–200 Ma) and Proterozoic grains comprise 39% and 6% of the remainder, respectively.

DISCUSSION

Provenance and Depositional History

All Nacimiento Franciscan sandstone groups contain abundant Cretaceous detrital zircon grains and significant proportions of lithic fragments plus plagioclase, confirming a probable Sierra Nevada–Peninsular Ranges arc source, as has been suggested previously (e.g., Dickinson et al., 1982; Ingersoll, 1983; Jacobson et al., 2011). Given the voluminous magmatism of the Sierran arc between ca. 120 and 80 Ma (e.g., Ducea, 2001) and the presence of Campanian microfossils in the Nacimiento Franciscan (Bailey et al., 1964; Evitt, 1967, written commun. *in* Hsü, 1969; Gilbert, 1971; Page, 1981; Hall, 1991), calculated maximum depositional ages from these sandstones probably closely reflect true sedimentary ages. Hence, in the discussion that follows, we assume that the variation in maximum depositional ages from Group 1 (ca. 95 ± 5 Ma) to Group 3 (ca. 82 ± 5 Ma) assemblages reflects a true difference in depositional age. However, it should be noted that Cenomanian–Coniacian forearc strata in the central Great Valley yield U-Pb zircon maximum depositional ages approximately 10–20 Ma older than the fossil-based depositional ages of these rocks (DeGraaff-Surpless et al., 2002; Sharman et al., 2015; Wakabayashi, 2015). We attribute this time lag between detrital zircon and actual depositional ages in the central Great Valley to the deposition of these rocks outboard of a Jurassic–Early Cretaceous arc segment. The depositional setting of these rocks resulted in a higher proportion of Jurassic–Early Cretaceous to Late Cretaceous zircon grains, a signature that we refer to in the section on the Origin of the Nacimiento Block as that of "central California." We now discuss the salient geochronologic and petrographic features of each group in order to clarify the Late Cretaceous evolution of the Nacimiento Franciscan.

Group 1

This group is characterized by abundant Cretaceous detrital zircon ages, particularly in the ca. 120–90 Ma range, few Jurassic and pre-Mesozoic grains, and a general lack of metamorphic recrystallization products, relative to other groups. Group 1A sandstones exhibit the oldest calculated maximum depositional ages of any group or subgroup (Figs. 5 and 8) and contain the highest proportions of lithic fragments, the majority of which are volcanic or polycrystalline quartz. Given the textural and mineralogical immaturity, relatively old maximum depositional ages, and essentially unimodal (ca. 100–120 Ma) detrital zircon age distributions of Group 1A samples, we interpret these rocks as some of the first clastic materials to have been delivered from the arc to the trench and accreted within the Nacimiento block. The lack of significant proportions of pre-Early Cretaceous grains strongly suggests a source for Group 1A detritus within the western Sierran-Peninsular Ranges magmatic arc, which at the time of deposition must have served as a topographic barrier, blocking craton interior debris from reaching the trench (e.g., Jacobson et al., 2011; Sharman et al., 2015).

In comparison with Group 1A sandstones, turbidite systems represented by Group 1B samples are ~5 m.y. younger, lack volcanic debris, contain significant chert and sedimentary lithic fragments, and are finer grained and more mature. Similar relations have led several workers to suggest that many Franciscan sandstones have a significant component reworked from earlier exhumed Franciscan rocks (e.g., Dickinson et al., 1982; Brothers and Grapes, 1989; Dumitru et al., 2015; Wakabayashi, 2015). Thus we suggest that Group 1B turbidites represent mixtures of arc-derived detritus and reworked siliciclastic material derived either from the growing accretionary prism or forearc basin and shed seaward from bathymetric highs on the subduction wedge (e.g., Bailleul et al., 2007). Following deposition, these turbidite systems probably remained perched on the wedge or were subducted to modest depths, as evidenced by their relative lack of deformation and secondary metamorphic minerals.

Group 2

In contrast to Group 1 assemblages, those of Group 2 are distributed along the entire length of the Nacimiento block and probably make up most of the volume of the Nacimiento wedge. Group 2A rocks yield maximum depositional ages that overlap those calculated from Group 1B. These groups differ in that Group 2A sandstones include more Jurassic and Late Cretaceous detrital zircon grains and are less mature, containing abundant volcanic fragments. These relations suggest increased delivery of first-cycle clastic detritus from the arc, across the trench-slope break, and into the Nacimiento trench. The observed influx of Late Cretaceous and Jurassic detrital zircon grains beginning at ca. 90 Ma suggests the input of material from farther inboard, most likely from the eastern Sierran-Peninsular Ranges arc, for the following reasons: (1) pluton ages in the arc are zoned from ca. 120–100 Ma in the west to ca. 100–80 Ma in the east, and (2) at the latitude of southern California, the eastern arc contains a higher proportion of intruded older arc segments, providing an explanation for the higher proportion of Jurassic grains in Group 2.

Group 2B assemblages record continued input of Jurassic grains into the trench after ca. 85 Ma, the maximum depositional age of this suite. Compared

with Group 2A, Group 2B rocks are more mature, containing relatively high proportions of quartz to feldspar plus lithic fragments (Fig. 4). Like Group 1B turbidites, Group 2B sandstones probably represent mixtures of reworked accretionary material and detritus sourced from the east and shed seaward.

Group 2 assemblages exhibit evidence for metamorphism under prehnite-pumpelleyite to blueschist-facies conditions. This observation, plus the paucity of metamorphic recrystallization products in older Group 1 samples, signals either: (1) a shift in the mode of accretion in the Nacimiento subduction complex from an early phase dominated by frontal accretion followed shortly thereafter by significant underplating and HP/LT metamorphism, or (2) a lack of exposure of underplated and metamorphosed Group 1 rocks.

Group 3 turbidite blocks in mélange comprise the youngest suite of accretionary rocks studied here, based on maximum depositional ages of ca. 82–86 Ma. Group 3 rocks contain similar detrital zircon age populations as, and are lithologically similar to, the Atascadero and Pigeon Point formations (Figs. 4 and 6), suggesting that Group 3 assemblages represent outboard facies equivalents of forearc strata. This group, including the Point San Luis slab, is also similar to the Type E Cambria and Pfeiffer slabs, containing minor detrital K-feldspar, lacking secondary metamorphic minerals and significant quantities of lithic fragments, and exhibiting overlapping detrital zircon age spectra (Figs. 4 and 6), though slabs contain more Jurassic and older grains. Of the lithic fragments present in these rocks, glaucophane schist comprises a minor component (Smith et al., 1979), indicating that HP/LT rocks were exhumed and exposed by ca. 82 Ma. In aggregate, the above observations suggest that these deposits represent mixtures of recycled trench and arc-derived detritus that never underwent deep subduction. Given that Group 3 assemblages crop out as blocks encased in mélange, plus the similarities between Group 3 and Cambria-Pfeiffer–Point San Luis slab deposits, we infer an olistostromal origin for this group, in which these assemblages were deposited and subsequently incorporated into the deforming wedge. Curiously, slabs and Group 3 deposits show significantly lower proportions of Jurassic and higher amounts of pre-Mesozoic grains relative to Group 2. The uptick in the proportion of Precambrian detrital zircon grains from Group 1 and Group 2 to Group 3 is likely the result of either (1) the latter group tapping shallow-water (miogeoclinal), passive-margin wall rocks in the eastern Sierra Nevada or (2) recycling Late Jurassic to Early Cretaceous forearc assemblages such as the Toro Formation, which contains significant populations of pre-Mesozoic and Jurassic detrital zircon grains (Johnston, 2013). Alternatively, it could be argued that incipient breachment of the Sierran-Peninsular Ranges topographic high occurred as Group 2 detritus was being shed into the trench. Such channelways would allow transport of Precambrian zircon-bearing detritus derived from the craton interior toward the margin. However, we consider this model unlikely, given that the detrital zircon-based signal for geomorphic breachment of the Cretaceous arc does not appear in the forearc until Maastrichtian time (e.g., Jacobson et al., 2011; Sharman et al., 2015).

A distinct source for Nacimiento Type E detritus is required given the presence of prominent age peaks at 1650–1800 Ma and ca. 1380 Ma. The Proterozoic age peak doublet exhibited by Type E rocks is unique and points to an ultimate source in central Idaho (Dumitru et al., 2016). The recognition of Type E detrital zircon distributions in Franciscan trench assemblages led Dumitru et al. (2016) to propose a ca. 80 Ma paleoriver that flowed southwest from Idaho to central California. The presence of Type E detritus in the Nacimiento Franciscan is explored further in the section that follows.

Group 3 rocks and Cambria-Pfeiffer–Point San Luis slabs crop out within ~5 km of the San Gregorio–Hosgri fault zone. We suggest that this apparent linear outcrop pattern, parallel to the strike of the Nacimiento belt, was due to wedge flexure adjacent to thrust faults (e.g., Smith et al., 1979). We propose that the proto–San Gregorio–Hosgri fault represents a Late Cretaceous intrawedge thrust fault, adjacent to which a trench-slope (e.g., Smith et al., 1979) or trench-axis (Ogawa et al., 2014) basin system developed, and that the fault reactivated in Neogene time as a strand of the San Andreas wrench system.

Slabs exposed west and east of the San Gregorio–Hosgri fault are commonly used as piercing points for constraining the magnitude of Neogene dextral slip along the fault (Smith et al., 1979; Hall, 1991; Dickinson et al., 2005). Estimates of Neogene dextral slip along this structure range widely from ~180 to <5 km (Sedlock and Hamilton, 1991; Burnham, 1998; Clark, 1998; Burnham, 1999; Dickinson et al., 2005). While constraining the magnitude of Neogene displacement along the San Gregorio–Hosgri fault is beyond the scope of this effort, our results showing similar distributions of detrital zircon ages in Pfeiffer and Point San Luis slabs support earlier correlations of these rocks and ~155 km of Neogene dextral slip along the San Gregorio–Hosgri fault (Dickinson et al., 2005).

Origin of the Nacimiento Block

Current models for Late Cretaceous–early Cenozoic slip along the Sur-Nacimiento fault include: (1) the fault is a thrust with ~150 km offset that placed Cretaceous batholithic rocks above the Cretaceous forearc basin and subduction complex outboard of the Mojave Desert (e.g., Page, 1970a, 1970b; Hall, 1991; Ducea et al., 2009); and (2) the fault is a sinistral tectonic escape structure with ~500–900 km offset that formed in response to collision of an aseismic ridge (e.g., Dickinson, 1983; Dickinson et al., 2005; Jacobson et al., 2011). The second model predicts that Nacimiento Franciscan and Great Valley Group assemblages originated outboard of the Diablo Range–San Francisco Bay Area in central California.

Distinguishing between an outboard southern versus central California origin for the Nacimiento block based on detrital zircon age distributions is challenging, given that each setting lies outboard of the Sierra Nevada batholith, which supplied significant amounts of Cretaceous zircon to the forearc and trench over >1000 km along strike. However, "central California" and "southern California" paleogeographic signatures may be distinguished based on the relative proportions of Jurassic plus Early Cretaceous to Late Cretaceous detrital zircon grain distributions. For example, the NNW-trending Late Cretaceous arc

was emplaced at an angle to the NW-trending, Jurassic–Early Cretaceous continental arc such that the older arc resides outboard of the younger in central California, and vice versa in southern California (e.g., Ernst, 2015; Sharman et al., 2015; Fig. 1 inset). As a result, a "central California" detrital zircon signal should include a relatively high proportion of Jurassic–Early Cretaceous to Late Cretaceous grains, given the position of the Jurassic–Early Cretaceous arc outboard of the Late Cretaceous arc, which likely represented a geomorphic barrier to detritus sourced from the continental interior. Underplated Rand-type schists in the southern Sierra Nevada–Salinia–Mojave Desert region show a "southern California" fingerprint (Barth et al., 2003; Grove et al., 2003; Jacobson et al., 2011; Chapman et al., 2013). Conversely, examples of trench and forearc assemblages with a "central California" signature include Franciscan rocks of the Diablo Range and San Francisco Bay area Franciscan rocks (Unruh et al., 2007; Ernst et al., 2009; Snow et al., 2010; Prohoroff et al., 2012) and the San Joaquin section of the Great Valley Group, near Coalinga (DeGraaff-Surpless et al., 2002; Jacobson et al., 2011; Sharman et al., 2015; Figs. 8 and 9).

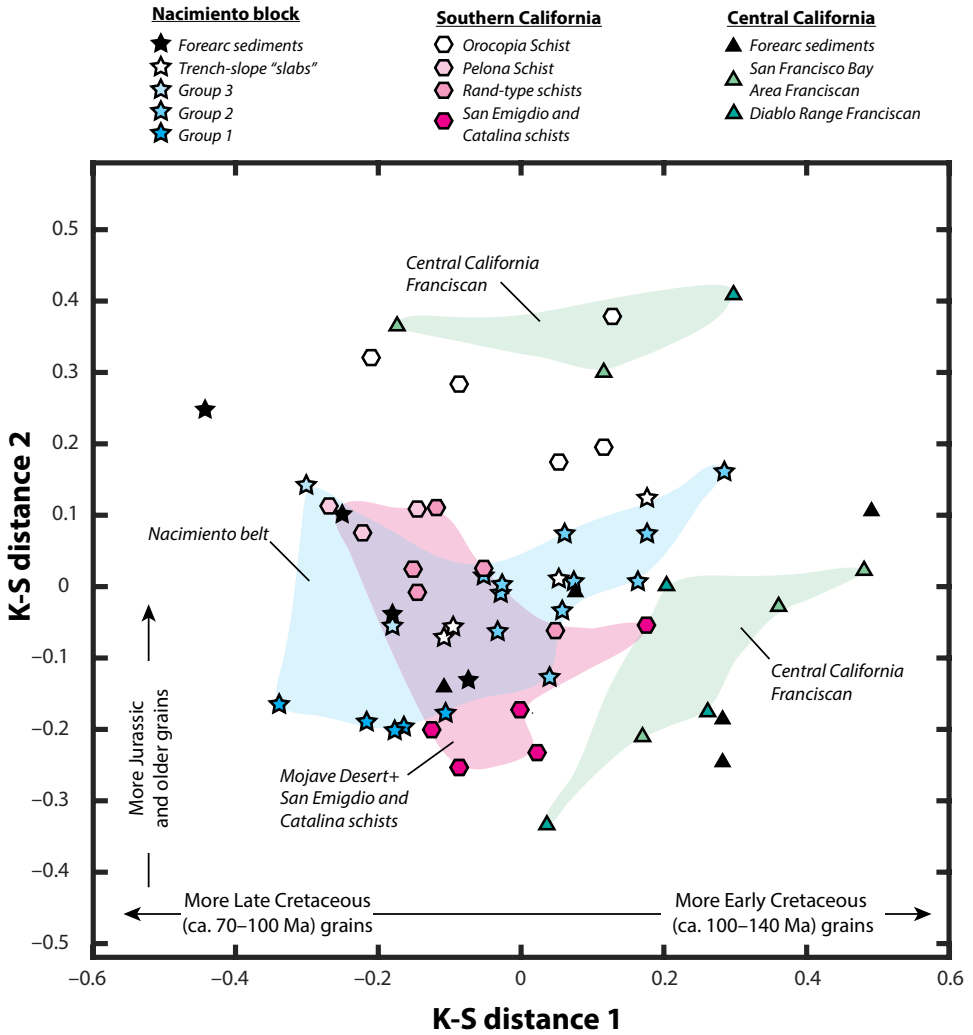

Figure 9. Multidimensional scaling map showing dimensionless Kolmogorov-Smirnov (K-S) distances between arrays of detrital zircon age data. See text for discussion. Data sources: Nacimiento Franciscan and forearc assemblages—Ernst et al. (2011), Jacobson et al. (2011), and this study; Diablo Range Franciscan—Unruh et al. (2007), Ernst et al. (2009), and this study; San Francisco Bay Area Franciscan—Snow et al. (2010); Rand-type schists—Barth et al. (2003), Grove et al. (2003), Jacobson et al. (2011), Chapman et al. (2013), and this study; Catalina Schist—Grove et al. (2008); Great Valley Group east of San Andreas fault—DeGraaff-Surpless et al. (2002) and Sharman et al. (2015).

Although central California Franciscan rocks generally yield "central California" type detrital zircon age spectra, these rocks show significant variability in age spectra, most likely due to the preservation of multiple thrust sheets and/or sedimentary recycling within the region. For example, one sample from a structurally low thrust sheet yields detrital zircon grains as young as ca. 52 Ma (Snow et al., 2010), while samples from higher structural levels yield maximum depositional ages as old as ca. 123 Ma (Prohoroff et al., 2012). Westward and structurally downward-younging patterns are commonly observed in the "type" Franciscan (e.g., Dumitru et al., 2015; Wakabayashi, 2015). In contrast, systematic spatial variations in detrital zircon age distributions are not observed in the Nacimiento Franciscan, although age distribution patterns do appear to fluctuate with time (Figs. 5, 6, 8, and 9). All four groups of Nacimiento rocks, plus Franciscan slabs and forearc assemblages of the Atascadero Formation, exhibit significantly higher proportions of Late Cretaceous to Jurassic–Early Cretaceous detrital zircon grains, and hence show "southern California" signatures. This observation supports an outboard Mojave origin for the Nacimiento block and is incompatible with the left-slip tectonic escape model.

As noted above, several samples in the Nacimiento Franciscan show Type E detrital zircon age spectra. This observation could be viewed as evidence supporting the left-slip model, given that Type E detrital zircon age spectra appear to be concentrated in Franciscan and Great Valley strata of central California (Dumitru et al., 2016). However, the schist of Sierra de Salinas, which accreted beneath southern California, also exhibits Type E zircon age arrays (Barth et al., 2003; Jacobson et al., 2011; Dumitru et al., 2016). Hence, the presence of such grains in subduction assemblages from both southern and central California cannot constrain the tectonic origin of the Nacimiento block. Type E spectra in the schist of Sierra de Salinas are explained by long-distance turbidite flow of sediment from central California down the trench axis (Dumitru et al., 2016). Furthermore, recent structural work by Ogawa et al. (2014) suggests that Nacimiento slabs may in fact represent trench axis deposits, not trench-slope deposits as traditionally interpreted, and so could receive detritus from Idaho in the same fashion as that invoked for the schist of Sierra de Salinas.

Relationship of Nacimiento Franciscan to Rand-Type Schists

As concluded above, the Nacimiento block likely originated outboard of southern California, where the Laramide shallow subduction (see footnote 1)–related, Late Cretaceous Rand-type, and early Cenozoic Pelona and Orocopia schists crop out (Graham and England, 1976; Haxel and Dillon, 1978; Ehlig, 1981; Jacobson, 1983, 1995; Jacobson et al., 1988, 2007, 2011; Simpson, 1990; Kidder and Ducea, 2006; Ducea et al., 2009; Chapman et al., 2010, 2011, 2012, 2013). The Nacimiento Franciscan and Late Cretaceous Rand-type schists are each elements of the subduction complex, contain similar proportions of metaclastic to metabasaltic rocks, exhibit strikingly similar detrital zircon age spectra with overlapping maximum depositional (ca. 95–80 Ma) and metamorphic (ca. 90–70 Ma) ages in metasandstones (Fig. 8), and originated adjacent to each other. The main difference between the Nacimiento Franciscan and Rand-type schists is metamorphic grade of metaclastic rocks, which generally ranges from sub-zeolite to prehnite-pumpelleyite facies in the former to greenschist to upper amphibolite facies in the latter (Ernst, 1980; Jacobson et al., 1988; Jacobson, 1995; Underwood et al., 1995; Underwood and Laughland, 2001; Kidder and Ducea, 2006; Chapman et al., 2011; Wakabayashi, 2015). These relations strongly suggest that the Rand, San Emigdio, and Sierra de Salinas schists represent high-grade equivalents to the Nacimiento Franciscan emplaced and exhumed from farther inboard. Group 1 and 2 assemblages exhibit similar detrital zircon age distributions to those of older schist members (e.g., Rand and Sierra de Salinas schists), whereas age spectra from Group 3 and trench-slope basin deposits more closely resemble those of the younger Pelona schist, implying possible correlations between these units (Figs. 8 and 9). Employing this logic, Nacimiento Franciscan rocks represent outboard (up-dip) elements of the Laramide shallow subduction (see footnote 1) system relative to Rand-type schists. Furthermore, the inboard remains of the Late Cretaceous subduction megathrust flat (locally the Rand fault and Salinas shear zone; Jacobson, 1995; Kidder and Ducea, 2006; Chapman et al., 2010) are analogous to the outboard Coast Range fault (Bailey et al., 1970; Platt, 1986; Jayko et al., 1987).

One of the most striking features of Rand-type schists is a pronounced shift in maximum depositional and metamorphic ages from >90 Ma in the northwest to <50 Ma in the southeast (Fig. 10). Given that the schist outcrop belt is oriented at a high angle (~30°) to the paleotrench, geographic variations in schist accretion age may be parallel, perpendicular, or at an intermediate angle to the continental margin. Models explaining spatial variations in schist age depend critically on the orientation of accretion "isochrons" with respect to the continental margin. For example, subduction erosion of upper-plate rocks plus progressive underplating of younger material farther inboard provides an attractive explanation for inboard schist younging (i.e., if isochrons are subparallel to the margin; Grove et al., 2003). On the other hand, oblique encroachment of an aseismic ridge with the margin and subsequent NW to SE time-transgressive collision would account for strike-parallel schist younging to the southeast (Barth and Schneiderman, 1996).

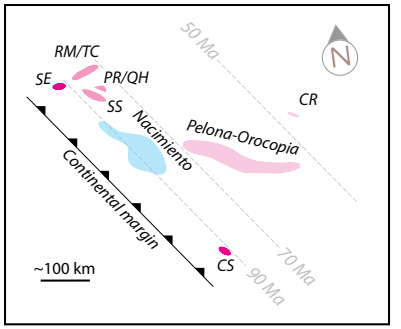

Figure 10. Schematic subduction erosion and underplating explanation for age variation within a sheet of Nacimiento Franciscan and Rand-type schist. Modified after Jacobson et al. (2011). Abbreviations: CR—Cemetery Ridge; CS—Catalina Schist; PR—Portal Ridge; QH—Quartz Hill; RM—Rand Mountains; SE—San Emigdio Mountains; TC—Tehachapi Mountains.

Palinspastic restoration of the Nacimiento Franciscan to its Late Cretaceous position outboard of the Mojave Desert provides critical constraints on this issue. In contrast to the schist outcrop belt, no clear relationship exists between calculated maximum depositional ages with position, strike parallel or perpendicular, along the Nacimiento Franciscan (Fig. 5). This observation is readily explained if accretion isochrons are oriented parallel to the strike of the Nacimiento block, which is only possible if they are also parallel to the continental margin. Hence, the consistency of maximum depositional ages in the Nacimiento Franciscan relative to the schist requires age variations to occur down dip, strongly suggesting a progressive subduction-erosion and underplating origin for regional age patterns (Fig. 11).

Evolution of Trench-Forearc-Arc System

As noted previously, the Nacimiento subduction-accretion package likely represents the outboard equivalents of Rand-type schists. In aggregate, the Nacimiento-schist accretionary package was assembled along a shallowly subducting (see footnote 1) segment of the Farallon slab that probably formed due to collision of an oceanic plateau with the continental margin (Saleeby, 2003; Liu et al., 2008, 2010). The plateau was consumed over a ~500-km-wide corridor between the southern Sierra Nevada and northern Peninsular Ranges (the southern California batholith) and is hypothesized to have driven slab flattening and tectonic removal of sub-batholithic mantle lithosphere, the cessation of arc magmatism, uplift and crustal thickening in the overriding plate, and structural ascent of batholithic assemblages from deep- to mid-crustal levels (Moxon and Graham, 1987; Malin et al., 1995; Ducea and Saleeby, 1998; House et al., 2001; Saleeby, 2003; Saleeby et al., 2007; Nadin and Saleeby, 2008; Chapman et al., 2010, 2012). The resulting uplifted mountain belt shed detritus (the Rand-type schists–Nacimiento belt protoliths) into the trench, which was immediately underthrust beneath the recently extinguished arc.

The replacement of sub-batholithic mantle with subduction-accretion assemblages resulting from shallow subduction (see footnote 1) marked a profound reduction in the strength of the southern California lithosphere. In response to regional lithospheric weakening, previously thickened and rootless orogenic crust collapsed under its own weight beginning ca. 75 Ma (Wood and Saleeby, 1997; Chapman et al., 2012; Hall and Saleeby, 2013). This event is marked by schist extrusion and dispersal of a series of extensional nappes, including Salinia, toward the continental margin (Chapman et al., 2010, 2012). The low-angle structures along which dispersal of upper-crustal fragments took place resemble, and have been interpreted previously as, out-of-sequence thrust faults (May, 1989), but are demonstrably extensional, placing upper-crustal granitic rocks on lower-crustal tonalitic rocks or directly on Rand-type schist (Wood and Saleeby, 1997; Chapman et al., 2012). This low-angle system, including Blackburn Canyon, Jawbone Canyon, and Pastoria faults, extends from the SE to the SW Sierra Nevada, where it is truncated by the San Andreas system (Fig. 1). This "southern Sierra detachment" is inferred between exposures of granitic and tonalitic rocks west of the San Andreas for ~50 km (James et al., 1993; Dickinson, 1996; Chapman et al., 2012; Fig. 1), after which its trace becomes unclear. We suggest the following alternative to thrust versus

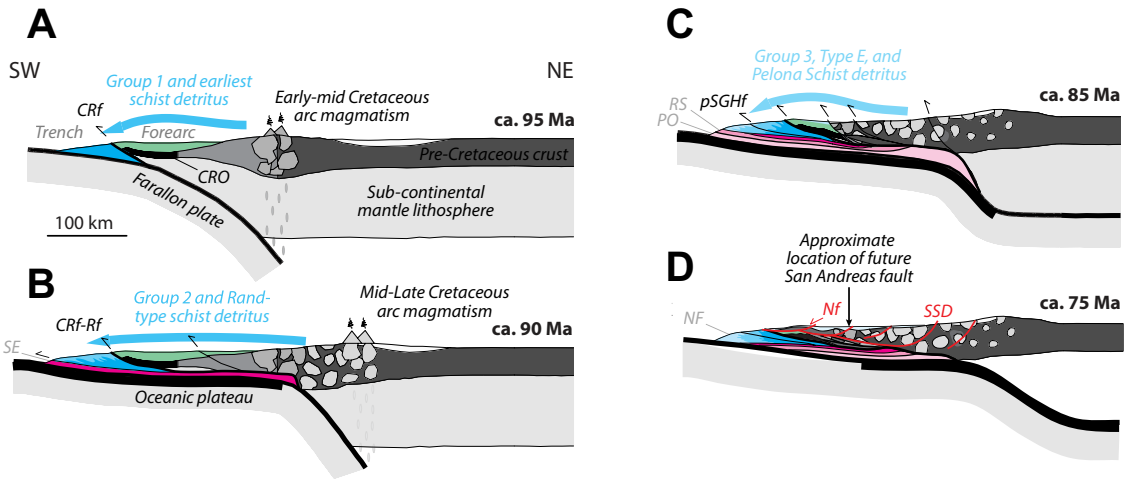

Figure 11. Model for development of the Sur-Nacimiento fault, modified after Jacobson et al. (2011). (A) Prior to shallow subduction (see footnote 1) showing magmatism in the western southern California batholith and deposition of Nacimiento Franciscan Group 1 and San Emigdio schist protoliths in the trench. (B) Onset of shallow subduction (see footnote 1) showing inboard migration of magmatism, upper plate thrusting and uplift, underplating of San Emigdio schist, and deposition of Nacimiento Franciscan Group 2 and Rand-type (includes Sierra de Salinas, Rand Mountains, Tehachapi Mountains, Portal Ridge, and Quartz Hill exposures) schist protoliths derived from farther-inboard sources. (C) Mature shallow subduction (see footnote 1) showing cessation of arc magmatism, intense upper plate contractile deformation including activity of the proto–San Gregorio–Hosgri fault, deposition and sequential underplating of Rand-type and later schists, and deposition of Nacimiento Group 3 and trench-slope basin deposits. (D) Waning shallow subduction (see footnote 1) and gravitational collapse and westward dispersal of upper-plate lithologies along the integrated southern Sierra detachment–Sur-Nacimiento fault system. Abbreviations: CRf—Coast Range fault; CRO—Coast Range Ophiolite; pSGHf—proto–San Gregorio–Hosgri fault; Nf—Nacimiento fault; NF—Nacimiento Franciscan; PO—Pelona and Orocopia schists; Rf—Rand fault; RS—Rand-type schists; SE—San Emigdio schist; SSD—southern Sierra detachment.

left-slip models for the Sur-Nacimiento fault: this fault, which juxtaposes Salinian block granitic rocks with trench assemblages, represents a segment of the southern Sierra detachment system. The observation that the Nacimiento fault was active between 75 and 56 Ma, synchronous with orogenic collapse in the southern Sierra Nevada–Mojave Desert–Salinia region (Chapman et al., 2012) and extension along the Coast Range fault (Platt, 1986; Jayko et al., 1987), lends additional support to an extensional origin for the Nacimiento fault. Extensional emplacement of the Salinian block must have covered the Nacimiento block to a modest degree (Fig. 11), providing an explanation for the post-Campanian depositional hiatus in the Nacimiento Great Valley Group and the widespread presence of Maastrichtian marine sediments in the Salinian block. This hypothesis also provides an intriguing explanation for the Big Creek "klippe" (Hall, 1991; Dickinson et al., 2005; Hall and Saleeby, 2013), which we interpret as an erosional remnant of extensional tectonostratigraphy.

Temporal variations in Nacimiento Franciscan detrital zircon populations support the above tectonic model, reflecting incipient oceanic plateau collision (Group 1), mature collision (Group 2), and incipient extensional collapse (Group 3, Type E, and Atascadero Formation) phases. We infer above that Group 1, Group 2, and Group 3 (plus Type E and Atascadero) detritus originated from the western Sierran-Peninsular Ranges magmatic arc and progressed to more easterly portions of the arc with time. This evolving provenance reflects: (1) the inboard migration of arc magmatism at the onset of shallow subduction (see footnote 1) (Group 1 to Group 2) to (2) magmatic arc collapse and dispersal of upper-crustal fragments such as the Salinian block to the SW at the end of shallow subduction (see footnote 1) (Group 2 to Group 3). By this interpretation, the absence of K-feldspar in Groups 1 and 2 assemblages and the presence of K-feldspar in Group 3 and trench-slope basin deposits probably reflects not only the degree of subduction, as traditionally interpreted (Gilbert, 1973; Hall, 1991; Underwood et al., 1995; Dickinson et al., 2005) but also the detrital source, given that the western arc is generally tonalitic (i.e., K-feldspar poor), whereas the eastern arc is more granitic.

Aside from the presence of Late Jurassic exotic blocks in mélange, the Nacimiento Franciscan apparently lacks accretionary materials older than ca. 95 Ma, indicating that the first >60 m.y. of subduction along the Rand-type margin was nonaccretionary, as is the case for approximately three-quarters of modern subduction zones (e.g., Scholl and von Huene, 2007; Dumitru et al., 2010). Construction of the Nacimiento–Rand-type schist wedge between ca. 95 and 80 Ma thus represents a profound shift toward accretionary behavior. This transition appears to be linked to collision and passage of the Laramide oceanic plateau beneath the southern California batholith, which dissected the formerly contiguous Sierran-Peninsular Ranges arc, and in doing so provided voluminous clastic sediment to the forearc region. Franciscan assemblages outside the Nacimiento block also display significant variations in accretion rate; but these took place chiefly in Early Cretaceous time (Dumitru et al., 2010; Ernst, 2011) and are tentatively attributed to changes in convergence vectors between North America and outboard oceanic plates (Engebretson et al., 1985; Seton et al., 2012).

Whither the Missing Forearc and Western Arc?

If the Nacimiento block is, as we suggest, a product of Laramide shallow subduction (see footnote 1), then why was the trench preserved while the forearc and western magmatic arc were apparently obliterated by oceanic plateau collision? In comparison with the trench-forearc-arc system preserved east of the San Andreas fault in central California, inner forearc and western arc elements are scarce in Late Cretaceous reconstructions of southern California (Page, 1981; Dickinson, 1983; Hall, 1991; James et al., 1993; Schott and Johnson, 1998; Schott et al., 2004; Dickinson et al., 2005; Jacobson et al., 2011; Chapman et al., 2012; Sharman et al., 2015). Were these elements subducted and recycled into the mantle, incorporated into the subduction complex, and/or displaced by margin-parallel strike slip? Based on abundant ca. 120–100 Ma detrital zircon grains, particularly in Group 1 assemblages, the local presence of tonalite clasts in the Nacimiento Franciscan (Cowan and Page, 1975; this study; Fig. 3), the generally intermediate composition of clastic rocks in the Nacimiento-schist belt, and the highly denuded state of western arc rocks directly above the Rand-type schist, we propose that a significant volume of inner forearc and disaggregated western arc domains resides within this belt.

The restored Nacimiento-schist belt is >400 km long (Sharman et al., 2015) and >200 km wide (Miller et al., 2000; Luffi et al., 2009; Haxel et al., 2015) and likely achieved a layer thickness between 10 and 30 km (Cheadle et al., 1986; Li et al., 1992; Malin et al., 1995; Porter et al., 2011). Thus, assuming a sheet-like geometry, the volume of clastic material accreted and subcreted to this belt was on the order of 1×10^6 km^3. Furthermore, this same belt has lost an ~150-km-wide wedge of arc plus forearc material that tapered from ~30 km arc thickness in the east (e.g., Gromet and Silver, 1987; Chapman et al., 2014) to <10 km ophiolite plus sediment thickness in the west (e.g., Jayko et al., 1987). These relations imply that the volume lost by removal of the inner forearc and western arc was comparable to the volume gain by emplacement of the Nacimiento-schist belt.

Although the above relations suggest that a substantial volume of disaggregated western magmatic arc and eastern forearc were interleaved in the subduction complex as clastic material, intact remnants of these elements still exist outside of the complex. A <5-km-thick interval of western arc (e.g., the Tehachapi–San Emigdio complex, Johannesburg Gneiss, Ben Lomond Mountain, Bodega Head, Montara Mountain, and Point Reyes) and forearc affinity (e.g., Coast Range Ophiolite and Toro Formation) rocks resides in a highly attenuated upper plate above the integrated Coast Range–Rand fault system (Seiders, 1982; Postlethwaite and Jacobson, 1987; Ross, 1989; James et al., 1993; Saleeby et al., 2007; Hopson et al., 2008; Chapman and Saleeby, 2012; Chapman et al., 2012; Sharman et al., 2015). The presence of these lithologies structurally above the Late Cretaceous subduction megathrust ~200 km inboard from the margin implies that a nontrivial amount of western arc material was carried to significant depths in the subduction zone by subduction erosion (Fig. 11).

We consider sinistral syn-subduction strike-slip removal of western arc and inner forearc domains unlikely, given the correlation drawn here between the Nacimiento Franciscan and the Rand-type schist and the apparent provenance

mismatch between the Nacimiento Franciscan and central California Franciscan assemblages. If western arc and inner forearc domains were translated away from southern California by Late Cretaceous strike slip, then they should be recognized somewhere along the continental margin. Inasmuch as the western arc and inner forearc are virtually nowhere to be seen, unless these elements are in the Peninsular Ranges (Dickinson, 1983), it is more likely that these rocks were removed by a combination of surficial erosion from above (and incorporation of this material into the subduction complex) and tectonic erosion from below (and subduction of this material into the mantle).

Constraints on the Origin of Nacimiento Mélange

The origin of mélange within the Nacimiento Franciscan, particularly in sea-cliff exposures near San Simeon (Fig. 2), has been debated since the pioneering work of Hsü (1968). Models for the incorporation of lithologically diverse fragments, including "exotic" blocks such as blueschist, in serpentinite or fine-grained siliciclastic material within the Nacimiento Franciscan fall generally into three categories: (1) *tectonic*—previously accreted blocks were plucked from the hanging wall of the subduction channel and exhumed by return flow (e.g., Cloos, 1982); (2) *sedimentary*—previously exhumed blocks and siliciclastic deposits slid down the trench slope and were (re)subducted (e.g., Cowan, 1978; Platt, 2015); and (3) *diapiric*—diapirs entrained blocks of subduction assemblages as they rose (e.g., Becker and Cloos, 1985; Ogawa et al., 2014). The latter model proposes that earlier formed tectonic mélange was reworked by diapirism; hence, we consider the diapiric model as a variation on the tectonic model.

Our detrital zircon results bear directly on the mélange issue. First, we document Group 1 and Group 2 assemblages as blocks in mélange, indicating that mélange formation must have taken place after ca. 85 Ma. Deposition of the Cambria slab, which contains detrital zircon grains as young as ca. 82 Ma and Campanian microfossils (Evitt, 1967, written commun. *in* Hsü, 1969; Hall, 1991; Jacobson et al., 2011), atop mélange provides a minimum age constraint on the timing of mélange formation. Hence, mélange in the vicinity of San Simeon must have formed in the Late Cretaceous and probably occurred within a narrow ca. 85–80 Ma window. Intrusion of mélange into the Cambria slab is well documented (e.g., Becker and Cloos, 1985; Ogawa et al., 2014) and must have taken place after this time interval.

Second, the sandstone block from which sample 11MB6 was collected is from the same mélange exposure where Ukar et al. (2012) determined ca. 154 Ma Ar-Ar ages on blueschist blocks. This sandstone block and others from the same area (Morisani, 2006) yield maximum depositional ages of ca. 85 Ma, indicating that at least 70 m.y. elapsed between the timing of blueschist-facies metamorphism in exotic blocks and deposition of sample 11MB6. Furthermore, no metamorphic index minerals were observed in this sample, indicating a significant contrast in metamorphic grade between blueschist blocks and the studied siliciclastic block. The highest-grade sandstone blocks exposed at San Simeon are of the prehnite-pumpelleyite facies (Cowan, 1978; Ernst, 1980). These observations may be explained in the framework of return flow if previously accreted rocks were plucked from a range of upper-plate locations as material flowed back out of trench and if the upper plate had cooled to lower-grade conditions (e.g., Cloos, 1982). However, there exists no structural evidence for trench-directed return flow (Cowan, 1978; Singleton and Cloos, 2013; Ogawa et al., 2014; Platt, 2015).

A simpler explanation for the observed differences in age and metamorphic grade between blueschist and siliciclastic blocks in San Simeon mélange is that both lithologies slid down the trench slope as debris flows and were incorporated together in a predominantly siliciclastic fine-grained matrix. This model is bolstered by the presence of detrital glaucophane in sandstone blocks at San Simeon (Cowan, 1978) and lithologically diverse blocks, including blueschist and granitic clasts, in conglomerate throughout the Nacimiento Franciscan (Hsü, 1969; Cowan and Page, 1975; this study), indicating that blueschist blocks must have been at the surface as siliciclastic rocks were deposited prior to mélange formation. Subsequent flattening and/or strike-slip tectonism within the subduction complex overprinted primary olistostrome features, resulting in strong deformational fabrics (Cowan, 1978; Singleton and Cloos, 2013; Platt, 2015). The >4 km (longest dimension) Group 1B turbidite block exposed south of Gorda (Fig. 2) probably also shares an olistostrome origin.

Additional support for the olistostrome model comes from the clear increase in compositional maturity in Nacimiento Franciscan lithologies with time (Fig. 4). This relationship strongly suggests progressive reworking of Nacimiento Franciscan assemblages in the accretionary system from ca. 95 to 80 Ma. An alternative explanation for the observed age-petrographic relationship may be progressive exposure of deeper levels of the Sierran-Peninsular Ranges arc with time so that the relative contribution of lithic fragments and feldspar decreases with time. Age-petrography trends in Great Valley Group sediments do indicate an increase in quartz relative to feldspar plus lithic fragments with time—but not nearly to the same extent as observed in the Nacimiento Franciscan (Fig. 4B). Hence, some amount of arc dissection is likely responsible for the age-maturity relationships observed in Nacimiento Franciscan, but significant recycling of exhumed clastic rocks must also be invoked to explain these relationships.

Given the age-maturity trends discussed above, sediment recycling in the Nacimiento accretionary system appears to have been operating on an ~10 m.y. timescale. It is not surprising that gravitational mélange formation occurred quickly in the Nacimiento Franciscan, from the perspective of accretionary wedge mechanics. The onset of Laramide shallow subduction (see footnote 1) would have been marked by a rapid decrease in slab dip and an increase in basal friction along the wedge–downgoing-slab interface. In order to maintain critical taper, the wedge would have had to increase its topographic slope (e.g., Davis et al., 1983). We argue that strata and previously exhumed high-grade mafic blocks perched on the trench slope were gravitationally destabilized by this slope increase and slid into the trench, where they were introduced to fine-grained siliciclastic matrix material.

CONCLUSIONS

Petrographic and U-Pb detrital zircon geochronologic relations presented here indicate that four distinct groups of siliciclastic subduction assemblages plus depositionally overlying trench-slope basin sediments were sourced from the southern California batholith to the east and comprise the basement of the Nacimiento block. Group 1 rocks contain abundant Middle Cretaceous (ca. 100–120 Ma) zircon grains with few older grains and yield the oldest maximum depositional ages ranging from ca. 98 to 90 Ma. Group 2 rocks are younger, with maximum depositional ages from ca. 93 to 85 Ma, and contain relatively abundant Late Cretaceous (ca. 80–100) and Early Cretaceous to Jurassic (ca. 120–200 Ma) zircon grains. Group 3 rocks yield maximum depositional ages of ca. 87–82 Ma and contain higher proportions of Precambrian zircon grains than Group 2 but lack Jurassic grains. Group 3 rocks contain similar detrital zircon age populations, are petrographically similar to trench-slope basin "slabs," and are interpreted here as slab materials incorporated in mélange through sedimentary processes. Group 3 and trench-slope basin rocks are, in turn, interpreted as distal equivalents to the Upper Cretaceous Atascadero Formation on the basis of petrographic and geochronologic similarities.

In aggregate, all Nacimiento sample groups, including trench-slope deposits, show a closer affinity to subduction-accretion assemblages exposed in southern California (e.g., the Sierra de Salinas, Rand, San Emigdio, and Pelona schists) than to Franciscan rocks exposed in central California (e.g., in the Diablo Range and San Francisco Bay Area). This observation supports the view that the Nacimiento block originated outboard of southern California (e.g., Hall, 1991; Ducea et al., 2009; Hall and Saleeby, 2013). In other words, models wherein the Nacimiento block originated outboard central California and was displaced >500 km to the south along a sinistral Sur-Nacimiento fault zone (e.g., Dickinson, 1983; Dickinson et al., 2005; Jacobson et al., 2011; Singleton and Cloos, 2013) are incompatible with the data presented here. Furthermore, the inference that Nacimiento assemblages likely represent outboard equivalents of Rand-type schists suggests that the Nacimiento Franciscan–Rand-type schist wedge represents an exhumed shallow subduction (see footnote 1) complex, the best known example of its kind. Recognition of the Nacimiento Franciscan as outboard schist equivalents suggests that NW-SE–younging trends in the schist were produced by subduction erosion, allowing progressively younger accretionary materials to "leap-frog" farther inboard (e.g., Grove et al., 2003), and probably did not result from time transgressive collision of an aseismic ridge (e.g., Barth and Schneiderman, 1996).

Siliciclastic assemblages in the Nacimiento Franciscan record the uplift, erosion, inboard migration of arc magmatism, and extensional collapse of the southern California batholith that accompanied Late Cretaceous collision and passage of an oceanic plateau beneath southern California (Wood and Saleeby, 1997; Saleeby, 2003; Liu et al., 2008, 2010; Chapman et al., 2012). We posit that a significant volume of inner forearc and western arc material, now absent from southern California, was eroded and interleaved in the shallow subduction (see footnote 1) complex. Mélange formation followed soon thereafter, most likely by incorporation of previously subducted materials plus first-cycle clastic detritus into a fine-grained siliciclastic matrix by submarine gravity sliding that accompanied wedge oversteepening due to shallow subduction (see footnote 1). A phase of regional extension followed assembly of the Nacimiento–Rand-type subduction complex, marked by slip along the integrated southern Sierra detachment–Nacimiento system and dispersal of upper-crustal fragments, including the Salinian block.

ACKNOWLEDGMENTS

This work was supported by National Science Foundation grant EAR-PF1250070 and a Richard Chambers Memorial Scholarship from the Northern California Geological Society (to ADC) and field support over many years by both the University of California, Los Angeles, and Stanford University (to WGE). The manuscript benefitted from editorial handling by R. Russo, thoughtful feedback by J. Singleton and an anonymous reviewer, and discussions and fieldwork with L. Arnold, G. Gehrels, G. Hartford, S. Johnston, J. Saleeby, A. Steely, J. Wakabayashi, and the GeoPRISMS ExTerra group. M. Coble is thanked for analytical assistance and for lending a rock hammer in a time of need.

REFERENCES CITED

Aalto, K.R., 2014, Examples of Franciscan Complex mélanges in the northernmost California Coast Ranges, a retrospective: International Geology Review, v. 56, p. 555–570, doi:10.1080/00206814.2013.879841.

Bailey, E.H., Irwin, W.P., and Jones, D.L., 1964, Franciscan and related rocks and their significance in the geology of western California: California Division of Mines and Geology Bulletin, v. 183, 177 p.

Bailey, E.H., Blake, M.C., Jr., and Jones, D.L., 1970, On-land Mesozoic oceanic crust in California Coast Ranges: U.S. Geological Survey Professional Paper 770C, p. C70–C81.

Bailleul, J., Robin, C., Chanier, F., Guillocheau, F., Field, B., and Ferrière, J., 2007, Turbidite systems in the inner forearc domain of the Hikurangi convergent margin (New Zealand): New constraints on the development of trench-slope basins: Journal of Sedimentary Research, v. 77, p. 263–283, doi:10.2110/jsr.2007.028.

Barth, A.P., and Schneiderman, J.S., 1996, A comparison of structures in the Andean orogen of northern Chile and exhumed midcrustal structures in southern California, USA: An analogy in tectonic style?: International Geology Review, v. 38, no. 12, p. 1075–1085, doi:10.1080/00206819709465383.

Barth, A.P., Wooden, J.L., Grove, M., Jacobson, C.E., and Pedrick, J.N., 2003, U-Pb zircon geochronology of rocks in the Salinas Valley region of California: A reevaluation of the crustal structure and origin of the Salinian Block: Geology, v. 31, no. 6, p. 517–520, doi:10.1130/0091-7613(2003)031<0517:UZGORI>2.0.CO;2.

Becker, D.G., and Cloos, M., 1985, Mélange diapirs into the Cambria Slab: A Franciscan trench slope basin near Cambria, California: The Journal of Geology, v. 93, p. 101–110, doi:10.1086/628934.

Berkland, J.O., Raymond, L.A., Kramer, J.C., Moores, E.M., and O'Day, M., 1972, What is Franciscan?: American Association of Petroleum Geologists Bulletin, v. 56, p. 2295–2302.

Black, L.P., Kamo, S.L., Allen, C.M., Davis, D.W., Aleinikoff, J.N., Valley, J.W., Mundil, R., Campbell, I.H., Korsch, R.J., Williams, I.S., and Foudoulis, C., 2004, Improved $^{206}Pb/^{238}U$ microprobe geochronology by the monitoring of a trace-element–related matrix effect; SHRIMP, ID-TIMS, ELA-ICP-MS and oxygen isotope documentation for a series of zircon standards: Chemical Geology, v. 205, no. 1–2, p. 115–140, doi:10.1016/j.chemgeo.2004.01.003.

Blake, M.C., Jr., Jayko, A.S., and McLaughlin, R.J., 1988, Metamorphic and tectonic evolution of the Franciscan Complex, northern California: p. 1035–1060, *in* Ernst, W.G., ed., Metamorphism and Crustal Evolution of the Western United States: Englewood Cliffs, New Jersey, Prentice-Hall,

Brothers, R.N., and Grapes, R.H., 1989, Clastic lawsonite, glaucophane, and jadeitic pyroxene in Franciscan metagraywackes from the Diablo Range, California: Geological Society of America Bulletin, v. 101, p. 14–26, doi:10.1130/0016-7606(1989)101<0014:CLGAJP>2.3.CO;2.

Burnham, K., 1998, Preliminary comparison and correlation of two Cretaceous conglomerates, the strata of Anchor Bay and an unnamed unit in the Pilarcitos block, across the San Gregorio and San Andreas faults, *in* Elder, W.P., ed., Geology and Tectonics of the Gualala Block, Northern California: Pacific Section, SEPM (Society for Sedimentary Geology), Book 84, p. 95–119.

Burnham, K., 1999, Stop #4—Point Lobos, comparison and correlation of Cretaceous and Paleogene rocks of Point Lobos and Point Reyes, *in* Garrison, R.E., Aiello, I.W., and Moore, J.C., eds., Late Cenozoic fluid seeps and tectonics along the San Gregorio fault zone in the Monterey Bay region, California: Pacific Section, American Association of Petroleum Geologists, Volume and Guidebook Book GB-76, p. 145–151.

Chapman, A.D., and Saleeby, J., 2012, Geologic map of the San Emigdio Mountains: Geological Society of America Map and Chart Series, v. MCH-101, 1:40,000 scale.

Chapman, A.D., Kidder, S., Saleeby, J.B., and Ducea, M.N., 2010, Role of extrusion of the Rand and Sierra de Salinas schists in Late Cretaceous extension and rotation of the southern Sierra Nevada and vicinity: Tectonics, v. 25, v. 5, p. 1–21.

Chapman, A.D., Luffi, P., Saleeby, J., and Petersen, S., 2011, Metamorphic evolution, partial melting, and rapid exhumation above an ancient flat slab: Insights from the San Emigdio Schist, southern California: Journal of Metamorphic Geology, v. 29, p. 601–626, doi:10.1111/j.1525–1314.2011.00932.x.

Chapman, A.D., Saleeby, J.B., Wood, D.J., Piasecki, A., Kidder, S., Ducea, M.N., and Farley, K.A., 2012, Late Cretaceous gravitational collapse of the southern Sierra Nevada batholith, California: Geosphere, v. 8, no. 2, p. 314–341, doi:10.1130/GES00740.1.

Chapman, A.D., Saleeby, J.B., and Eiler, J.M., 2013, Slab flattening trigger for isotopic disturbance and magmatic flare-up in the southernmost Sierra Nevada batholith: California Geology, v. 41, p. 1007–1010, doi:10.1130/G34445.1.

Chapman, A.D., Ducea, M.N., Kidder, S., and Petrescu, L., 2014, Geochemical constraints on the petrogenesis of the Salinian arc, central California: Implications for the origin of intermediate magmas: Lithos, v. 200–201, p. 126–141, doi:10.1016/j.lithos.2014.04.011.

Chapman, A.D., Ernst, W.G., Gottlieb, E., Powerman, V., and Metzger, E., 2015, Detrital zircon geochronology of Neoproterozoic–Lower Cambrian passive margin strata of the White-Inyo Range, east-central California: Implications for the Mojave–Snow Lake fault hypothesis: Geological Society of America Bulletin, doi:10.1130/B31142.1.

Cheadle, M.J., Czuchra, B.L., Byrne, T., Ando, C.J., Oliver, J.E., Brown, L.D., Kaufman, S., Malin, P.E., and Phinney, R.A., 1986, The deep crustal structure of the Mojave Desert, California, from COCORP seismic reflection data: Tectonics, v. 5, p. 293–320, doi:10.1029/TC005i002p00293.

Chen, J.H., and Moore, J.G., 1982, Uranium-lead isotopic ages from the Sierra Nevada batholith, California: Journal of Geophysical Research, v. 87, p. 4761–4784, doi:10.1029/JB087iB06p04761.

Clark, J.C., 1998, Neotectonics of the San Gregorio fault zone: Age dating controls on offset history and slip rates: American Association of Petroleum Geologists Bulletin, v. 82, p. 884–885.

Cloos, M., 1982, Flow mélanges: Numerical modeling and geologic constraints on their origin in the Franciscan subduction complex, California: Geological Society of America Bulletin, v. 93, p. 330–345. doi:10.1130/0016-7606(1982)93<330:FMNMAG>2.0.CO;2.

Cowan, D.S., 1974, Deformation and metamorphism of the Franciscan subduction zone complex northwest of Pacheco Pass, California: Geological Society of America Bulletin, v. 85, p. 1623–1634, doi:10.1130/0016-7606(1974)85<1623:DAMOTF>2.0.CO;2.

Cowan, D.S., 1978, Origin of blueschist-bearing chaotic rocks in the Franciscan Complex, San Simeon, California: Geological Society of America Bulletin, v. 89, p. 1415–1423, doi:10.1130/0016-7606(1978)89<1415:OOBCRI>2.0.CO;2.

Cowan, D.S., and Page, B.M., 1975, Recycled Franciscan material in Franciscan mélange west of Paso Robles, California: Geological Society of America Bulletin, v. 86, p. 1089–1095. doi:10.1130/0016-7606(1975)86<1089:RFMIFM>2.0.CO;2.

Davis, D., Suppe, J., and Dahlen, F.A., 1983, Mechanics of fold- and-thrust belts and accretionary wedges: Journal of Geophysical Research, v. 88, p. 1153–1172, doi:10.1029/JB088iB02p01153.

DeGraaff-Surpless, K., Graham, S.A., Wooden, J.L., and McWilliams, M.O., 2002, Detrital zircon provenance analysis of the Great Valley Group, California: Evolution of an arc-forearc system: Geological Society of America Bulletin, v. 114, p. 1564–1580. doi:10.1130/0016-7606(2002)114<1564:DZPAOT>2.0.CO;2.

Dibblee, T.W., 1966, Geology of the Central Santa Ynez Mountains, Santa Barbara County, California: California Division of Mines and Geology Bulletin, v. 186, p. 186.

Dibblee, T.W., Jr., 1971, Geologic maps of seventeen 15-minute quadrangles (1:62,500) along the San Andreas fault in the vicinity of King City, Coalinga, Panoche Valley, and Paso Robles, California, with index map: U.S. Geological Survey Open-File Report 71-0087, 17 sheets, scale 1:62,500.

Dibblee, T.W., 2007, Geologic map of the Villa Creek and Burro Mountain quadrangles, San Luis Obispo and Monterey counties, California, Santa Barbara, California: Santa Barbara Museum of Natural History, scale 1:24,000.

Dickinson, W.R., 1983, Cretaceous sinistral strike slip along the Nacimiento fault in coastal California: American Association of Petroleum Geologists Bulletin, v. 67, p. 624–645.

Dickinson, W.R., 1996, Kinematics of transrotational tectonism in the California Transverse Ranges and its contribution to cumulative slip along the San Andreas transform fault system: Geological Society of America Special Paper 305, 46 p.

Dickinson, W.R., and Gehrels, G.E., 2009, U-Pb ages of detrital zircons in Jurassic eolian and associated sandstones of the Colorado Plateau: Evidence for transcontinental dispersal and intraregional recycling of sediment: Geological Society of America Bulletin, v. 121, p. 408–433, doi:10.1130/B26406.1.

Dickinson, W.R., and Suczek, C.A., 1979, Plate tectonics and sandstone compositions: American Association of Petroleum Geologists Bulletin, v. 63, p. 2164–2182.

Dickinson, W.R., Ingersoll, R.V., Cowan, D.S., Helmold, K.P., and Suczek, C.A., 1982, Provenance of Franciscan graywackes in coastal California: Geological Society of America Bulletin, v. 93, p. 95–107, doi:10.1130/0016-7606(1982)93<95:POFGIC>2.0.CO;2.

Dickinson, W.R., Ducea, M., Rosenberg, L.I., Greene, H.G., Graham, S.A., Clark, J.C., Weber, G.E., Kidder, S., Ernst, W.G., and Brabb, E.E., 2005, Net dextral slip, Neogene San Gregorio–Hosgri fault zone, coastal California: Geologic evidence and tectonic implications: Geological Society of America Special Paper 391, 43 p., doi:10.1130/2005.2391.

Ducea, M., 2001, The California arc: Thick granitic batholiths, eclogitic residues, lithospheric-scale thrusting, and magmatic flare-ups: GSA Today, v. 11, no. 11, p. 4–10, doi:10.1130/1052-5173 (2001)011<0004:TCATGB>2.0.CO;2.

Ducea, M.N., and Saleeby, J.B., 1998, The age and origin of a thick mafic-ultramafic keel from beneath the Sierra Nevada Batholith: Contributions to Mineralogy and Petrology, v. 133, p. 169–185, doi:10.1007 /s004100050445.

Ducea, M.N., Kidder, S., Chesley, J.T., and Saleeby, J.B., 2009, Tectonic underplating of trench sediments beneath magmatic arcs: The central California example: International Geology Review, v. 51, no. 1, p. 1–26, doi:10.1080/00206810802602767.

Dumitru, T.A., Wright, J.E., Wakabayashi, J., and Wooden, J.L., 2010, Early Cretaceous (ca. 123 Ma) transition from nonaccretionary behavior to strongly accretionary behavior within the Franciscan subduction complex: Tectonics, v. 29, p. TC5001, doi:10.1029/2009TC002542.

Dumitru, T.A., Ernst, W.G., Hourigan, J.K., and McLaughlin, R.J., 2015, Detrital zircon U-Pb reconnaissance of the Franciscan accretionary complex in northwestern California: International Geology Review, v. 57, p. 767–800, doi:10.1080/00206814.2015.1008060.

Dumitru, T. A., Elder, W. P., Hourigan, J. K., Chapman, A. D., Graham, S. A., and Wakabayashi, J., 2016, Four Cordilleran paleorivers that connected Sevier thrust zones in Idaho to depocenters in California, Washington, Wyoming, and, indirectly, Alaska: Geology, v. 44, p. 75–78, doi:10.1130/G37286.1.

Ehlig, P.L., 1981, Origin and tectonic history of the basement terrane of the San Gabriel Mountains, central Transverse Ranges, *in* Ernst, W.G., ed., The Geotectonic Development of California, Rubey Volume I: New Jersey, Prentice-Hall, p. 253–283.

Engebretson, D.C., Cox, A., and Gordon, R.G., 1985, Relative motion between oceanic and continental plates in the Pacific basin: Geological Society of America Special Paper 206, 59 p.

Ernst, W.G., 1970, Tectonic contact between the Franciscan mélange and the Great Valley Sequence, crustal expression of a Late Mesozoic Benioff Zone: Journal of Geophysical Research, v. 75, p. 886–901, doi:10.1029/JB075i005p00886.

Ernst, W.G., 1980, Mineral paragenesis in Franciscan metagraywackes of the Nacimiento Block, a subduction complex of the Southern California Coast Ranges: Journal of Geophysical Research, v. 85, p. 7045–7055, doi:10.1029/JB085iB12p07045.

Ernst, W.G., 1993, Metamorphism of Franciscan tectonostratigraphic assemblage, Pacheco Pass area, east-central Diablo Range, California Coast Ranges: Geological Society of America Bulletin, v. 105, p. 618–636, doi:10.1130/0016-7606(1993)105<0618:MOFTAP>2.3.CO;2.

Ernst, W.G., 2011, Accretion of the Franciscan Complex attending Jura-Cretaceous geotectonic development of northern and central California: Geological Society of America Bulletin, v. 123, p. 1667–1678, doi:10.1130/B30398.1.

Ernst, W.G., 2015, Franciscan geologic history constrained by tectonic/olistostromal high-grade metamafic blocks in the iconic California Mesozoic–Cenozoic accretionary complex: The American Mineralogist, v. 100, p. 6–13, doi:10.2138/am-2015-4850.

Ernst, W. G., Martens, U., and Valencia, V., 2009, U-Pb ages of detrital zircons in Pacheco Pass metagraywackes: Sierran-Klamath source of mid- and Late Cretaceous Franciscan deposition and underplating: Tectonics, v. 28, TC6011, doi:10.1029/2008TC002352.

Ernst, W.G., Martens, U.C., McLaughlin, R.J., Clark, J.C., and Moore, D.E., 2011, Zircon U-Pb age of the Pescadero felsite: A Late Cretaceous igneous event in the forearc, west-central California Coast Ranges: Geological Society of America Bulletin, v. 123, p. 1497–1512, doi: 10.1130/B30270.1.

Gehrels, G., Valencia, V., and Pullen, A., 2006, Detrital zircon geochronology by laser-ablation multicollector ICPMS at the Arizona Laserchron Center: The Paleontological Society Papers, v. 12, p. 67–76.

Gehrels, G., Valencia, V.A., and Ruiz, J., 2008, Enhanced precision, accuracy, efficiency, and spatial resolution of U-Pb ages by laser ablation–multicollector–inductively coupled plasma–mass spectrometry: Geochemistry Geophysics Geosystems, v. 9, no. 3, doi:10.1029 /2007GC001805.

Gilbert, W.G., 1971, Sur fault zone, Monterey County, California [Ph.D. dissertation]: Stanford, California, Stanford University, 80 p.

Gilbert, W.G., 1973, Franciscan Rocks near Sur Fault Zone, Northern Santa Lucia Range, California: Geological Society of America Bulletin, v. 84, p. 3317–3328, doi:10.1130/0016-7606 (1973)84<3317:FRNSFZ>2.0.CO;2.

Gilbert, W.G., and Dickinson, W.R. 1970, Stratigraphic variations in sandstone petrology, Great Valley sequence, central California coast: Geological Society of America Bulletin, v. 81, p. 949–954, doi:10.1130/0016-7606(1970)81[949:SVISPG]2.0.CO;2.

Graham, C.M., and England, P.C., 1976, Thermal regimes and regional metamorphism in the vicinity of overthrust faults: An example of shear heating and inverted metamorphic zonation from southern California: Earth and Planetary Science Letters, v. 31, no. 1, p. 142–152, doi:10.1016/0012-821X(76)90105-9.

Gromet, L.P., and Silver, L.T., 1987, REE variations across the Peninsular Ranges Batholith: Implications for batholithic petrogenesis and crustal growth in magmatic arcs: Journal of Petrology, v. 28, p. 75–125, doi:10.1093/petrology/28.1.75.

Grove, M., Jacobson, C.E., Barth, A.P., and Vucic, A., 2003, Temporal and spatial trends of Late Cretaceous–early Tertiary underplating of Pelona and related schist beneath southern California and southwestern Arizona, *in* Johnson, S.E., Patterson, S.R., Fletcher, J.M., Girty, G.H., Kimbrough, D.L., and Martin-Barajas, A., eds., Tectonic Evolution of Northwestern Mexico and the Southwestern USA: Boulder, Colorado, Geological Society of America Special Paper 374, p. 381–406.

Grove, M., Bebout, G.E., Jacobson, C.E., Barth, A.P., Kimbrough, D.L., King, R.L., Zou, H., Lovera, O.M., Mahoney, B.J., and Gehrels, G.G., 2008, The Catalina schist: Evidence for middle Cretaceous subduction erosion of southwestern North America, *in* Draut, A.E., Clift, P.D., and Scholl, D.W., eds., Formation and Applications of the Sedimentary Record in Arc Collision Zones: Geological Society of America Special Paper 436, p. 335–362.

Hall, C.A., Jr., 1981, Map of geology along the Little Pine fault, parts of the Sisquoc, Foxen Canyon, Zaca Lake, Bald Mountain, Los Olivos, and Figureroa Mountain Quadrangles, Santa Barbara County, California: U.S. Geological Survey Miscellaneous Field Studies Map MF-1285, scale 1:24,000.

Hall, C.A., Jr., 1991, Geology of the Point Sur–Lopez Point region, Coast Ranges, California: A part of the Southern California allochthon: Geological Society of America Special Paper 266, 44 p.

Hall, C.A., Jr., and Saleeby, J., 2013, Salinia revisited: A crystalline nappe sequence lying above the Nacimiento fault and dispersed along the San Andreas fault system, central California: International Geology Review, v. 55, no. 13, p. 1575–1615, doi:10.1080/00206814.2013.825141.

Hall, C.A., Jr., Ernst, W.G., Prior, S.W., and Wiese, J.W., 1979, Geologic map of the San Luis Obispo–San Simeon region, California: U.S. Geological Survey Miscellaneous Investigations Series Map I-1097, scale 1:48,000 (3 sheets).

Hamilton, W.B., 1969, Mesozoic California and the underflow of Pacific mantle: Geological Society of America Bulletin, v. 80, p. 2409–2430. doi:10.1130/0016-7606(1969)80[2409:MCATUO]2 .0.CO;2.

Haxel, G., and Dillon, J., 1978, The Pelona-Orocopia Schist and Vincent–Chocolate Mountain thrust system, southern California, *in* Howell, D.G., and McDougall, K.A., eds., Mesozoic Paleogeography of the Western United States: Pacific Section, Society of Economic Paleontologists and Mineralogists Pacific Coast Paleogeography Symposium 2, p. 453–469.

Haxel, G.B., Jacobson, C.E., and Wittke, J.H., 2015, Mantle peridotite in newly discovered far-inland subduction complex, southwest Arizona: Initial report: International Geology Review, v. 57, p. 871–892, doi:10.1080/00206814.2014.928916.

Hernandez, J.L., 2010, Geologic map of the Lancaster West 7.5′ quadrangle, Los Angeles County, California: A digital database: California Geological Survey, Preliminary Geologic Maps, scale 1:24,000.

Hopson, C.A., Mattinson, J.M., Pessagno, E.A., Jr., and Luyendyk, B.P., 2008, California Coast Range Ophiolite: Composite Middle and Late Jurassic oceanic lithosphere, *in* Wright, J.E., and Shervais, J.W., eds., Ophiolites, Arcs, and Batholiths: A Tribute to Cliff Hopson: Geological Society of America Special Paper 483, p. 1–101.

Hornafius, J.S., Luyendyk., B.P, Terres, R.R., and Kamerling, M.J., 1986; Timing and extent of Neogene tectonic rotation in the western Transverse Ranges, California: Geological Society of America Bulletin, v. 97, p. 1476–1487.

House, M.A., Wernicke, B.P., and Farley, K.A., 2001, Paleogeomorphology of the Sierra Nevada, California, from (U-Th)/He ages in apatite: American Journal of Science, v. 301, no. 2, p. 77–102, doi:10.2475/ajs.301.2.77.

Hsü, K.J., 1968, The principles of mélanges and their bearing on the Franciscan-Knoxville paradox: Geological Society of America Bulletin, v. 79, p. 1063–1074, doi:10.1130/0016-7606 (1968)79[1063:POMATB]2.0.CO;2.

Hsü, K.J., 1969, Preliminary report and geologic guide to Franciscan mélanges of the Morro Bay–San Simeon area, California: California Division of Mines and Geology Special Publication 35, 46 p.

Ingersoll, R. V., 1978, Petrofacies and petrologic evolution of the Late Cretaceous forearc basin, northern and central California: Journal of Geology, v. 86, p. 335–352.

Ingersoll, R.V., 1983, Petrofacies and provenance of late Mesozoic fore-arc basin, northern and central California: American Association of Petroleum Geologists Bulletin, v. 67, p. 1125–1142.

Irwin, W.P., and Barnes, I., 1975, Effect of geologic structure and metamorphic fluids on seismic behavior of the San Andreas fault system in central and northern California: Geology, v. 3, no. 12, p. 713–716, doi:10.1130/0091-7613(1975)3<713:EOGSAM>2.0.CO;2.

Jacobson, C.E., 1983, Structural geology of the Pelona Schist and Vincent Thrust, San Gabriel Mountains, California: Geological Society of America Bulletin, v. 94, no. 6, p. 753–767, doi:10 .1130/0016-7606(1983)94 <753:SGOTPS>2.0.CO;2.

Jacobson, C.E., 1995, Qualitative thermobarometry of inverted metamorphism in the Pelona and Rand schists, southern California, using calciferous amphibole in mafic schist: Journal of Metamorphic Geology, v. 13, no. 1, p. 79–92, doi:10.1111/j.1525-1314.1995 .tb00206.x.

Jacobson, C.E., Dawson, M.R., and Postlethwaite, C.E., 1988, Structure, metamorphism, and tectonic significance of the Pelona, Orocopia, and Rand schists, southern California, *in* Ernst, W.G., ed., Metamorphism and Crustal Evolution of the Western United States, Rubey Volume 7: New Jersey, Prentice-Hall, p. 976–997.

Jacobson, C.E., Oyarzabal, F.R., and Haxel, G.B., 1996, Subduction and exhumation of the Pelona-Orocopia-Rand schists, southern California: Geology, v. 24, p. 547–550, doi:10.1130/0091 -7613(1996)024<0547:SAEOTP>2.3.CO;2.

Jacobson, C.E., Grove, M., Vucic, A., Pedrick, J.N., and Ebert, K.A., 2007, Exhumation of the Orocopia Schist and associated rocks of southeastern California: Relative roles of erosion, synsubduction tectonic denudation, and middle Cenozoic extension: Geological Society of America Special Paper, v. 419, p. 1–37.

Jacobson, C.E., Grove, M., Pedrick, J.N., Barth, A.P., Marsaglia, K.M., Gehrels, G.E., and Nourse, J.A., 2011, Late Cretaceous–early Cenozoic evolution of the southern California margin inferred from provenance of trench and forearc sediments: Geological Society of America Bulletin, v. 123, no. 3–4, p. 485–506.

Jacobson, M.I., 1978, Petrologic variations in Franciscan sandstone from the Diablo Range, California, *in* Howell, D. G., and McDougall, K. A., eds., Mesozoic paleogeography of the western United States: Society of Economic Paleontologists and Mineralogists, Pacific Section, Pacific Coast Paleogeography Symposium 2, p. 401–417.

James, E.W., Kimbrough, D.L., and Mattinson, J.M., 1993, Evaluation of displacements of pre-Tertiary rocks on the northern San Andreas fault using U-Pb zircon dating, initial Sr, and common Pb isotopic ratios: Geological Society of America, v. 178, p. 257–272, doi:10.1130 /MEM178-p257.

Jayko, A.S., and Blake, M.C., Jr., 1993, Northward displacement of forearc slivers in the Coast Ranges of California and southwest Oregon during the late Mesozoic and early Cenozoic, *in* Dunn, G., and McDougall, K., eds., Mesozoic Paleogeography of the Western United States—II: Los Angeles, California, Pacific Section Society of Economic Paleontologists and Mineralogists, v. 71, p. 19–36.

Jayko, A.S., Blake, M.C., Jr., and Harms, T., 1987, Attenuation of the Coast Range Ophiolite by extensional faulting, and nature of the Coast Range "Thrust," California: Tectonics, v. 6, p. 475–488, doi:10.1029/TC006i004p00475.

Jayko, A.S., Blake, M.C., Jr., McLaughlin, R.J., Ohlin, H.N., Ellen, S.D., and Kelsey, H., 1989, Reconnaissance geologic map of the Covelo 30- by 60-minute quadrangle, northern California: U.S. Geological Survey Miscellaneous Field Studies Map, MF-2001, scale 1:100,000.

Johnston, S., 2013, Detrital zircon geochronology and geochemistry of the Nacimiento block, central California Coast: Geological Society of America Abstracts with Programs, v. 45, no. 7, p. 519.

Kidder, S., and Ducea, M.N., 2006, High temperatures and inverted metamorphism in the schist of Sierra de Salinas, California: Earth and Planetary Science Letters, v. 241, no. 3–4, p. 422–437, doi:10.1016/j.epsl.2005.11.037.

Kimbrough, D.L., Grove, M., and Morton, D.M., 2014, Timing and significance of gabbro emplacement within two distinct plutonic domains of the Peninsular Ranges batholith, southern and Baja California: Geological Society of America Bulletin, doi:10.1130/B30914.1.

Korsch, R.J., 1982, Structure of Franciscan Complex in the Stanley Mountain window, southern Coast Ranges, California: American Journal of Science, v. 282, p. 1406–1437, doi:10.2475/ajs.282.9.1406.

Lee-Wong, F., and Howell, D.G., 1977, Petrography of Upper Cretaceous sandstones in the Coast Ranges of California, *in* Howell, D.G., Vedder, J.G., and McDougall, K., eds., Cretaceous geology of the California Coast Ranges west of the San Andreas fault: Pacific Section, SEPM (Society for Sedimentary Geology), Pacific Coast Paleogeography Field Guide 2, p. 47–55.

Li, Y.G., Henyey, T.L., and Silver, L.T., 1992, Aspects of the crustal structure of the western Mojave Desert, California, from seismic reflection and gravity data: Journal of Geophysical Research, v. 97, p. 8805–8816, doi:10.1029/91JB02119.

Liu, L., Spasojevic, S., and Gurnis, M., 2008, Reconstructing Farallon plate subduction beneath North America back to the Late Cretaceous: Science, v. 322, p. 934–938, doi:10.1126/science.1162921.

Liu, L., Gurnis, M., Seton, M., Saleeby, J., Muller, R.D., and Jackson, J., 2010, The role of oceanic plateau subduction in the Laramide orogeny: Nature Geoscience, v. 3, p. 353–357, doi:10.1038/ngeo829.

Ludwig, K.R., 2003, Mathematical-statistical treatment of data and errors for ^{230}Th/U geochronology: Reviews in Mineralogy and Geochemistry, v. 52, p. 631–656, doi:10.2113/0520631.

Luffi, P., Saleeby, J.B., Lee, C.A., and Ducea, M.N., 2009, Lithospheric mantle duplex beneath the central Mojave Desert revealed by xenoliths from Dish Hill, California: Journal of Geophysical Research, v. 114, p. B03202, doi:10.1029/2008JB005906.

Luyendyk, B.P., 1991, A model for Neogene crustal rotations, transtension, and transpression in southern California: Geological Society of America Bulletin, v. 103, p. 1528–1536, doi:10.1130/0016-7606(1991)103<1528:AMFNCR>2.3.CO;2.

Mackinnon, T.C., 1978, The Great Valley sequence near Santa Barbara, California, *in* Howell, D.G., and McDougall, K.A., eds., Mesozoic paleogeography of the western United States: Society of Economic Paleontologists and Mineralogists, Pacific Section, Pacific Coast Paleogeography Symposium 2, p. 483–491.

Malin, P. E., Goodman, E. D., Henyey, T. L., Li, Y. G., Okaya, D. A., and Saleeby, J. B., 1995, Significance of seismic reflections beneath a tilted exposure of deep continental crust, Tehachapi Mountains, California: Journal of Geophysical Research, v. 100, no. B2, p. 2069–2087, doi:10.1029/94JB02127.

Mansfield, C.F., 1979, Upper Mesozoic subsea fan deposits in the southern Diablo Range, California: Record of the Sierra Nevada magmatic arc: Geological Society of America Bulletin, v. 90, p. 1025–1046, doi:10.1130/0016-7606(1979)90<1025:UMSFDI>2.0.CO;2.

Mattinson, J.M., and Echeverria, L.M., 1980, Ortigalita Peak Gabbro, Franciscan Complex: U-Pb ages of intrusion and high pressure-low temperature metamorphism: Geology, v. 8, p. 589–593, doi:10.1130/0091-7613(1980)8<589:OPGFCU>2.0.CO;2.

May, D.J., 1989, Late Cretaceous intra-arc thrusting in southern California: Tectonics, v. 8, no. 6, p. 1159–1173, doi:10.1029/TC008i006p01159.

McLaughlin, R.J., Blake, M.C., Jr., Griscom, A., Blome, C.D., and Murchey, B., 1988, Tectonics of formation, translation and dispersal of the Coast Range ophiolite of California: Tectonics, v. 7, p. 1033–1056, doi:10.1029/TC007i005p01033.

McLaughlin, R.J., Sliter, W.V., Frederiksen, N.O., Harbert, W.P., and McCulloch, D.S., 1994, Plate motions recorded in tectonostratigraphic terranes of the Franciscan Complex and evolution of the Mendocino triple junction, northwestern California: U.S. Geological Survey Bulletin 1997, 60 p.

McLaughlin, R.J., Ellen, S.D., Blake, M.C., Jr., Jayko, A.S., Irwin, W.P., Aalto, K.R., Carver, G.A., Clarke, S.H., Jr., Barnes, J.B., Cecil, J.D., and Cyr, K.A., 2000, Geology of the Cape Mendocino, Eureka, Garberville, and southwestern part of the Hayfork 30 × 60 minute quadrangles and adjacent offshore area, including a digital database: U.S. Geological Survey Miscellaneous Field Studies Map MF-2336, scale 1:137,000.

Miller, J.S., Glazner, A.F., Farmer, G.L., Suayah, I.B., and Keith, L.A., 2000, A Sr, Nd and Pb isotopic study of mantle domains and crustal structure from Miocene volcanic rocks of the Mojave Desert, California: Geological Society of America Bulletin, v. 112, p. 1264–1279, doi:10.1130/0016-7606(2000)112<1264:ASNAPI>2.0.CO;2.

Morisani, A.M., 2006, Detrital zircon geochronology and petrography of Franciscan graywacke blocks at San Simeon, California: Implications for mélange genesis [M.S. thesis]: Austin, Texas, The University of Texas at Austin, 391 p.

Moxon, I.W., and Graham, S.A., 1987, History and controls of subsidence in the Late Cretaceous–Tertiary Great Valley forearc basin, California: Geology, v. 15, p. 626–629, doi:10.1130/0091-7613(1987)15<626:HACOSI>2.0.CO;2.

Nadin, E.S., and Saleeby, J.B., 2008, Disruption of regional primary structure of the Sierra Nevada Batholith by the Kern Canyon fault system, California: Geological Society of America Special Paper 438, p. 429–454.

Nadin, E.S., Saleeby, J.B., and Wong, M., 2016 Thermal evolution of the Sierra Nevada batholith, California, and implications for strain localization: Geosphere, v. 12, doi:10.1130/GES01221.1 (in press).

Ogawa, Y., Mori, R., and Tsunogae, T., 2014, New interpretation of Franciscan mélange at San Simeon coast, California: Tectonic intrusion into an accretionary prism: International Geology Review, doi:10.1080/00206814.2014.968813.

Page, B.M., 1970a, Sur-Nacimiento fault zone of California: Continental margin tectonics: Geological Society of America Bulletin, v. 81, no. 3, p. 667–690, doi:10.1130/0016-7606(1970)81[667:SFZOCC]2.0.CO;2.

Page, B.M., 1970b, Time of completion of underthrusting of Franciscan beneath Great Valley rocks west of Salinian block, California: Geological Society of America Bulletin, v. 81, no. 9, p. 2825–2834, doi:10.1130/0016-7606(1970)81[2825:TOCOUO]2.0.CO;2.

Page, B.M., 1972, Oceanic crust and mantle fragment in subduction complex near San Luis Obispo, California: Geological Society of America Bulletin, v. 83, p. 957–972, doi:10.1130/0016-7606(1972)83[957:OCAMFI]2.0.CO;2.

Page, B.M., 1981, The southern Coast Ranges, *in* Ernst, W.G., ed., The Geotectonic Development of California, Rubey Volume I: Englewood Cliffs, New Jersey, Prentice-Hall, p. 329–417.

Paton, C., Hellstrom, J.C., Paul, B., Woodhead, J.D., and Hergt, J.M., 2011, Iolite: Freeware for the visualisation and processing of mass spectrometric data: Journal of Analytical Atomic Spectrometry, v. 26, p. 2508–2518, doi:10.1039/c1ja10172b.

Platt, J.P., 1986, Dynamics of orogenic wedges and the uplift of high-pressure metamorphic rocks: Geological Society of America Bulletin, v. 97, p. 1037–1053, doi:10.1130/0016-7606(1986)97<1037:DOOWAT>2.0.CO;2.

Platt, J.P., 2015, Origin of Franciscan blueschist-bearing melange at San Simeon, central California Coast: International Geology Review, v. 57, p. 843–853, doi:10.1080/00206814.2014.902756.

Porter, R., Zandt, G., and McQuarrie, N., 2011, Pervasive lower-crustal seismic anisotropy in Southern California: Evidence for underplated schists and active tectonics: Lithosphere, v. 3, p. 201–220, doi:10.1130/L126.1.

Postlethwaite, C.E., and Jacobson, C.E., 1987, Early history and reactivation of the Rand thrust, southern California: Journal of Structural Geology, v. 9, no. 2, p. 195–205, doi:10.1016/0191-8141(87)90025-3.

Prohoroff, R.E., Wakabayashi, J., and Dumitru, T.A., 2012, Sandstone-matrix olistostrome deposited on intra-subduction complex serpentinite, Franciscan Complex, western Marin County, California: Tectonophysics, v. 568–569, p. 296–305, doi:10.1016/j.tecto.2012.05.018.

Raymond, L.A., 1984, Classification of mélanges, *in* Raymond, L.A., ed., Mélanges: Their Nature, Origins, and Significance: Geological Society of America Special Paper 198, p. 7–20.

Ross, D.C., 1989, The metamorphic and plutonic rocks of the southernmost Sierra Nevada, California, and their tectonic framework: U.S. Geological Survey Professional Paper 1381, 159 p.

Saleeby, J., 2003, Segmentation of the Laramide slab—Evidence from the southern Sierra Nevada region: Geological Society of America Bulletin, v. 115, p. 655–668, doi:10.1130/0016-7606(2003)115<0655:SOTLSF>2.0.CO;2.

Saleeby, J.B., and Dunne, G., 2015, Temporal and tectonic relations of early Mesozoic arc magmatism, southern Sierra Nevada, California: Geological Society of America Special Paper 513, doi:10.1130/2015.2513(05).

Saleeby, J., Farley, K.A., Kistler, R.W., and Fleck, R.J., 2007, Thermal evolution and exhumation of deep-level batholithic exposures, southernmost Sierra Nevada, California: Geological Society of America Special Paper 419, p. 39–66.

Schmitz, M.D., Bowring, S.A., and Ireland, T.R., 2003, Evaluation of Duluth complex anorthositic series (AS3) zircon as a U-Pb geochronological standard: New high-precision isotope dilution thermal ionization mass spectrometry results: Geochimica et Cosmochimica Acta, v. 67, p. 3665–3672, doi:10.1016/S0016-7037(03)00200-X.

Scholl, D.W., and von Huene, R., 2007, Crustal recycling at modern subduction zones applied to the past—Issues of growth and preservation of continental basement crust, mantle geochemistry, and supercontinent reconstruction, *in* Hatcher, R.D., Jr., Carlson, M.P., McBride, J.H., and Martinez Catalán, J.R., eds., 4D Framework of Continental Crust: Boulder, Colorado, Geological Society of America Memoir 200, p. 9–33.

Schott, R.C., and Johnson, C.M., 1998, Sedimentary record of the Late Cretaceous thrusting and collapse of the Salinia-Mojave magmatic arc: Geology, v. 26, no. 4, p. 327–330, doi:10.1130/0091-7613(1998)026 <0327:SROTLC>2.3.CO;2.

Schott, R.C., Johnson, J.M., and O'Neil, J.R., 2004, Late Cretaceous tectonic history of the Sierra-Salinia-Mojave arc as recorded in conglomerates of the Upper Cretaceous and Paleocene Gualala Formation, northern California: Journal of Geophysical Research, v. 109, B02204, doi: 10.1029/ 203JB002845, 22 p.

Sedlock, R.L., and Hamilton, D.H., 1991, Late Cenozoic tectonic evolution of southwestern California: Journal of Geophysical Research, v. 96, p. 2325–2351, doi:10.1029/90JB02018.

Seiders, V.M., 1982, Geologic map of an area near York Mountain, California: U.S. Geological Survey Miscellaneous Investigations Map I-1396, scale 1: 24,000.

Seiders, V.M., 1983, Correlation and provenance of upper Mesozoic chert-rich conglomerate of California: Geological Society of America Bulletin, v. 94, p. 875–888, doi:10.1130/0016-7606(1983)94<875:CAPOUM>2.0.CO;2.

Seton, M., Müller, R.D., Zahirovic, S., Gaina, C., Torsvik, T., Shephard, G., Talsma, A., Gurnis, M., Turner, M., and Chandler, M., 2012, Global continental and ocean basin reconstructions since 200 Ma: Earth-Science Reviews, v. 113, p. 212–270, doi:10.1016/j.earscirev.2012.03.002.

Sharman, G.R., Graham, S.A., Grove, M., and Hourigan, J.K., 2013, A reappraisal of the early slip history of the San Andreas fault, central California, USA: Geology, v. 41, p. 727–730, doi:10.1130/G34214.1.

Sharman, G.R., Graham, S.A., Grove, M., Kimbrough, D.L., and Wright, J.E., 2015, Detrital zircon provenance of the Late Cretaceous–Eocene California forearc: Influence of Laramide low-angle subduction on sediment dispersal and paleogeography: Geological Society of America Bulletin, doi:10.1130/B31065.1.

Sharry, J., 1981, The geology of the western Tehachapi mountains, California [Ph.D. thesis]: Cambridge, Massachusetts Institute of Technology, 215 p.

Simpson, C., 1990, Microstructural evidence for northeastward movement on the Chocolate Mountains fault zone, southeastern California: Journal of Geophysical Research, v. 95, B1, p. 529–537, doi:10.1029 /JB095iB01p00529.

Singleton, J.S., and Cloos, M., 2013, Kinematic analysis of mélange fabrics in the Franciscan Complex near San Simeon, California: Evidence for sinistral slip on the Nacimiento fault zone?: Lithosphere, v. 5, p. 179–188, doi:10.1130/L259.1.

Smith, G.W., 1978, Stratigraphy, sedimentology, and petrology of the Cambria slab, San Luis Obispo County, California [M.S. thesis]: Albuquerque, New Mexico, University of New Mexico, 123 p.

Smith, G.W., Howell, D.G., and Ingersoll, R.V., 1979, Late Cretaceous trench-slope basins of central California: Geology, v. 7, p. 303–306, doi:10.1130/0091-7613(1979)7<303:LCTBOC>2.0.CO;2.

Snow, C.A., Wakabayashi, J., Ernst, W.G., and Wooden, J.L., 2010, Detrital zircon evidence for progressive underthrusting in Franciscan metagraywackes, west-central California: Geological Society of America Bulletin, v. 122, p. 282– 291. doi:10.1130/B26399.1.

Suppe, J., and Armstrong, R.L., 1972, Potassium-argon dating of Franciscan metamorphic rocks: American Journal of Science, v. 272, p. 217–233, doi:10.2475/ajs.272.3.217.

Ukar, E., 2012, Tectonic significance of low-temperature blueschist blocks in the Franciscan mélange at San Simeon, California: Tectonophysics, v. 568–569, p. 154–169, doi:10.1016/j.tecto.2011.12.039.

Ukar, E., Cloos, M., and Vasconcelos, P., 2012, First ^{40}Ar-^{39}Ar ages from low-T mafic blueschist blocks in a Franciscan mélange near San Simeon: Implications for initiation of subduction: The Journal of Geology, v. 120, p. 543–556, doi:10.1086/666745.

Underwood, M.B., and Howell, D.G., 1987, Thermal maturity of the Cambria slab, an inferred trench-slope basin in central California: Geology, v. 15, p. 216–219, doi:10.1130/0091-7613(1987)15<216:TMOTCS>2.0.CO;2.

Underwood, M.B., and Laughland, M.B., 2001, Paleothermal structure of the Point San Luis slab of central California: Effects of Late Cretaceous underplating, out-of-sequence thrusting, and late Cenozoic dextral offset: Tectonics, v. 20, p. 97–111, doi:10.1029/1999TC001153.

Underwood, M.B., Laughland, M.B., Shelton, K.L., and Sedlock, R.L., 1995, Thermal-maturity trends within Franciscan rocks near Big Sur, California: Implications for offset along the San Gregorio–San Simeon– Hosgri fault zone: Geology, v. 23, p. 839–842, doi:10.1130/0091-7613(1995)023<0839:TMTWFR>2.3.CO;2.

Unruh, J.R., Dumitru, T.A., and Sawyer, T.L., 2007, Coupling of early Tertiary extension in the Great Valley forearc basin with blueschist exhumation in the underlying Franciscan accretionary wedge at Mount Diablo, California: Geological Society of America Bulletin, v. 119, p. 1347–1367, doi:10.1130/B26057.1.

Vermeesch, P., 2013, Multi-sample comparison of detrital age distributions: Chemical Geology, v. 341, p. 140–146, doi:10.1016/j.chemgeo.2013.01.010.

Wakabayashi, J., 1999, Distribution of displacement on, and evolution of, a young transform fault system: The northern San Andreas fault system, California: Tectonics, v. 18, p. 1245–1274, doi:10.1029/1999TC900049.

Wakabayashi, J., 2015, Anatomy of a subduction complex: Architecture of the Franciscan Complex, California, at multiple length and time scales: International Geology Review, v. 57, p. 669–746, doi:10.1080/00206814.2014.998728.

Wills, C.J., Manson, M.W., Brown, K.D., Davenport, C.W., and Domrose, C.J., 2001, Landslides in the Highway 1 Corridor: Geology and Slope Stability along the Big Sur Coast between Point Lobos and San Carpoforo Creek, Monterey and San Luis Obispo Counties, California: California Department of Transportation Project F99TL34.

Wood, D.J., and Saleeby, J.B., 1997, Late Cretaceous– Paleocene extensional collapse and disaggregation of the southernmost Sierra Nevada Batholith: International Geology Review, v. 39, no. 11, p. 973–1009, doi:10.1080/00206819709465314.